P1.84

A FULLY-IMPLICIT SEMI-LAGRANGIAN HYDROSTATIC MODEL OF ATMOSPHERIC DYNAMICS

Sajal K. Kar[i]
I.M. Systems Group, Inc., Kensington, MD

1. INTRODUCTION

In a numerical model of the atmosphere, a time-difference scheme is needed to discretize the governing equations in time and thereby make a prediction of the future state of the atmosphere. The computational efficiency of a hydrostatic numerical model is commonly dictated by the size of the time step it can take, without violating the so-called Courant-Friedrichs-Lewy, or CFL, linear-computational stability condition on the fastest moving external gravity-wave solution of the governing primitive equations. In case of fully-explicit time-difference schemes that are second-order accurate in time, this implies that the Courant number associated with the external wave-mode must be typically less than one half. Thus, a relatively large number of time steps would be needed by such schemes to complete the forecast.

As opposed to the fully-explicit time-difference schemes, the semi-implicit and semi-Lagrangian (SISL) schemes applied to the hydrostatic primitive equations, treat the external and internal gravity wave-modes in a time-implicit manner, and treat the relatively slow advective processes in a semi-Lagrangian manner. The SISL scheme is nearly stable unconditionally, thus, significantly larger time steps compared to a fully-explicit time-difference scheme can be used in the model, generally resulting in a significant computational economy. The pioneering studies of Dr André Robert in the development of SISL methods and subsequent application of such methods in designing atmospheric numerical models have been duly recognized by many authors in a memorial volume (Lin et al. 1997).

An inherent weakness of the SISL schemes lies in the fact that certain terms of the governing equations that are non-advective (thus not stabilized by semi-Lagrangian advection scheme) and not responsible for gravity-wave propagation (thus not stabilized by semi-implicit scheme), are treated in a time-explicit manner. This reduces the robustness of the SISL scheme and the SISL model would then require additional stability measures when relatively large time steps are used. The model also becomes sensitive towards the choice of the reference thermodynamic profile that is used to 'linearize' the governing equations for implementation of the semi-implicit scheme.

To alleviate these problems associated with the SISL schemes, a fully-implicit semi-Lagrangian (FISL) scheme for the hydrostatic primitive equations has been developed. The FISL scheme presented here is set in a horizontally two-dimensional (2D) semi-Lagrangian framework, with all processes other than horizontal advection treated in a time-implicit manner. The semi-implicit linearization of the governing equations, followed up by a vertical decoupling of the gravity-wave eigen-modes of the system, results in a fully-implicit system that is solved iteratively. A set of 2D Helmholtz-type elliptic equations, one for each vertical eigen-mode, forms the Kernel of the implicit system. The 2D elliptic equations are then solved iteratively by a generalized conjugate residual (GCR) algorithm (e.g., Saad 2003). Recently, a fully-implicit, semi-Lagrangian, nonhydrostatic, global grid-point model has been developed by Yeh et al. (2002).

The use of a 2D semi-Lagrangian (SL) framework rather than a three-dimensional (3D) semi-Lagrangian framework for the proposed FISL formulation, is preferred because the 2D trajectory computations and 2D horizontal interpolations are relatively less expensive compared to their 3D counter parts. However, nothing precludes us from using 3D trajectories in place of 2D trajectories in the formulation. Specifically for this reason, the 2D SL-

formulation of FISL is derived as an extension of the 3D SL-formulation in the text.

The hydrostatic primitive equations employed in our model is based on a terrain following hydrostatic-pressure based vertical coordinate, that assumes a constant pressure at the model top. Thus, it is a modified form of Phillips' (1957) σ-coordinate. The equations are discretized in the vertical using a staggered Lorenz grid. Horizontally, the equations are cast in conformal-map coordinates, and discretization is carried out on an unstaggered A grid. This particular choice of horizontal grid is computationally convenient for the 2D semi-Lagrangian advection scheme employed here. In terms of the choice of spatial grids and space discretizations, and subsequent derivation of the implicit system of equations, the FISL scheme developed here bears close resemblance with the 2D SISL hydrostatic, grid-point model developed by Kar and Logan (2000) at the Bureau of Meteorology Research Centre (BMRC), Melbourne, Australia.

In section 2, we present the formulation of the FISL hydrostatic model. The results from numerical integrations of the model are presented in section 3. In the final section, we present some conclusions.

2. MODEL FORMULATION

a. The governing equations in a continuous form

The governing equations for a hydrostatic, moist-diabatic atmosphere can be written in a generalized vertical coordinate (η):

Momentum equations

$$d_t u = f_z v - m[R_d T_v(\partial_x \ln \tilde{p})_\eta + (\partial_x \Phi)_\eta] + F_x \,, \quad (2.1)$$

$$d_t v = -f_z u - m[R_d T_v(\partial_y \ln \tilde{p})_\eta + (\partial_y \Phi)_\eta] + F_y \,, \quad (2.2)$$

Mass continuity equation

$$d_t \ln\left|\partial_\eta \tilde{p}\right| + D + \partial_\eta \dot{\eta} = 0, \quad (2.3)$$

Thermodynamic energy equation

$$d_t T - \kappa_d \frac{T_v}{1+(\delta-1)q} d_t \ln \tilde{p} = Q/c_{pd} \,, \quad (2.4)$$

Moisture continuity equation

$$d_t q = -Q_2 / L \,, \quad (2.5)$$

Hydrostatic equation

$$\partial_\eta \Phi + R_d T_v \partial_\eta \ln \tilde{p} = 0 \,, \quad (2.6)$$

where

$$d_t \equiv \partial_t + mu\partial_x + mv\partial_y + \dot{\eta}\partial_\eta \,, \quad (2.7a)$$

$$f_z \equiv f + u\partial_y m - v\partial_x m \,, \quad (2.7b)$$

$$f \equiv 2\Omega \sin\varphi \,, \quad (2.7c)$$

$$D \equiv m^2[\partial_x(u/m) + \partial_y(v/m)] \,, \quad (2.7d)$$

$$T_v \equiv T\left[1 + (\varepsilon^{-1} - 1)q\right], \quad (2.7e)$$

$$\varepsilon \equiv R_d/R_v \,;\ \delta \equiv c_{pv}/c_{pd} \,;\ \kappa_d \equiv R_d/c_{pd} \,. \quad (2.7f)$$

Here (x, y) denote the Cartesian conformal map-projection horizontal coordinates with the map factor m; u and v denote the velocity components in the x and y directions, respectively, with the associated horizontal divergence D; $\dot{\eta}$ denotes the η-coordinate vertical velocity. T, q, and T_v, denote the temperature, specific humidity, and virtual temperature, respectively; $\tilde{p}$ and Φ denote the hydrostatic pressure and the geopotential (gz), respectively; (F_x, F_y) denote the friction terms in (u, v) momentum equations, respectively; Q in (2.4) denotes the heating rate; Q_2 and L in (2.5) respectively denote the apparent moisture sink and the latent heat of condensation. The numerous physical constants have their usual meaning.

In this model, the vertical coordinate (η) is chosen to be a terrain-following coordinate based on $\tilde{p}$; the model top is assumed to be a constant-pressure surface ($\tilde{p} = p_T$) and let $\tilde{p}_S(x, y, t)$ denote the surface pressure. Then, η is defined by

$$\eta = \frac{\tilde{p}_S - \tilde{p}}{\tilde{p}_S - p_T} \,. \quad (2.8)$$

This shows that from the surface to model top, η varies from 0 to 1. The surface and the model top are assumed to be material surfaces, so the lower and the upper boundary conditions on $\dot{\eta}$ are given by

$$\dot{\eta} = 0 \ \text{ at } \ \eta = 0 \ \text{ and } \ \eta = 1 \,. \quad (2.9)$$

For later convenience, we introduce the variables Π and Λ,

$$\Pi \equiv \tilde{p}_S - p_T \,, \quad (2.10a)$$

$$\Lambda \equiv \ln \Pi \,. \quad (2.10b)$$

Then, from (2.8) and (2.10a), we obtain

$$\tilde{p} = \tilde{p}_S - \eta(\tilde{p}_S - p_T) = p_T + (1-\eta)\Pi \,, \quad (2.11a)$$

and

$$-\partial_\eta \tilde{p} = \Pi\,. \tag{2.11b}$$

Notice that with the current choice of η, $-\partial_\eta \tilde{p}$ becomes independent of η.

b. Manipulation of the governing equations

Let us now rewrite the governing equations so that the fully-implicit (or semi-implicit) semi-Lagrangian (FISL or SISL) space- and time-difference schemes can be readily implemented later. (From now on, we omit the 'physics' terms from the governing equations, assuming such terms are added up later in a 'time-split' manner.) To start, using (2.11b) and (2.10b), we can rewrite *the mass-continuity equation* (2.3) as

$$d_t \Lambda + D + \partial_\eta \dot{\eta} = 0\,. \tag{2.3}'$$

Or

$$\boxed{d_t \Lambda = -(D + \partial_\eta \dot{\eta}) \equiv F_\Lambda}. \tag{2.12}$$

Note that including (2.12) above, the most relevant equations derived later in the text, are all enclosed in boxes for ease of reference.

Let us assume an isothermal reference atmosphere with the constant temperature, T_0. Then, the *thermodynamic energy equation* (2.4) is trivially rewritten in the form:

$$d_t (T - \kappa_d T_0 \Lambda) = \kappa_d \left[\frac{T_v}{1 + (\delta - 1)q} d_t \ln \tilde{p} - T_0 F_\Lambda \right], \tag{2.4}'$$

where (2.12) has been used in the right-hand side (rhs) of (2.4)′. Moreover, using (2.10), (2.11a), (2.7a), and (2.12), we can rewrite the $d_t \ln \tilde{p}$ term in the rhs of (2.4)′, as

$$\begin{aligned} d_t \ln \tilde{p} &= \frac{1}{\tilde{p}} d_t (\tilde{p} - p_T) \\ &= \frac{\tilde{p} - p_T}{\tilde{p}} d_t \ln(\tilde{p} - p_T) \\ &= \left(1 - \frac{p_T}{\tilde{p}}\right) d_t \ln[(1-\eta)\Pi]. \end{aligned} \tag{2.13}$$

Or

$$\begin{aligned} d_t \ln \tilde{p} &= \left(1 - \frac{p_T}{\tilde{p}}\right)[d_t \ln(1-\eta) + d_t \Lambda] \\ &= \left(1 - \frac{p_T}{\tilde{p}}\right)\left[-\frac{\dot{\eta}}{1-\eta} + F_\Lambda\right]. \end{aligned} \tag{2.13}'$$

Then, using (2.13)′ in (2.4)′, the thermodynamic energy equation is *finally* expressed as

$$\boxed{\begin{aligned} &d_t (T - \kappa_d T_0 \Lambda) = \\ &\kappa_d \left[\frac{T_v}{1 + (\delta - 1)q} \left(1 - \frac{p_T}{\tilde{p}}\right) \left(F_\Lambda - \frac{\dot{\eta}}{1-\eta}\right) \right. \\ &\qquad \left. - T_0 F_\Lambda \right] \equiv F_T\,. \end{aligned}} \tag{2.14}$$

Next, the *horizontal momentum equations* (2.1) and (2.2) are rewritten as

$$\boxed{\begin{aligned} &d_t u = \\ &f_z v - m[R_d T_v (\partial_x \ln \tilde{p})_\eta + (\partial_x \Phi)_\eta] \equiv F_u \end{aligned}}, \tag{2.15a}$$

$$\boxed{\begin{aligned} &d_t v = \\ &-f_z u - m[R_d T_v (\partial_y \ln \tilde{p})_\eta + (\partial_y \Phi)_\eta] \equiv F_v \end{aligned}}. \tag{2.15b}$$

We ignore the moisture continuity equation (2.5) until later, and proceed with the *hydrostatic equation* (2.6) instead. Let us first simplify the $\partial_\eta \ln \tilde{p}$ term in (2.6). Using (2.11a), we obtain

$$\begin{aligned} \ln \tilde{p} &= \ln[p_T + (1-\eta)\Pi] \\ &= \ln(1-\eta) + \ln[\tilde{p}/(1-\eta)] \end{aligned}, \tag{2.16}$$

so that (2.6) reduces to

$$\begin{aligned} &\partial_\eta \Phi = \\ &-R_d T_v [\partial_\eta \ln(1-\eta) + \partial_\eta \ln\{\tilde{p}/(1-\eta)\}]. \end{aligned} \tag{2.6}'$$

Vertically integrating (2.6)′ from the surface ($\eta = 0$, $\Phi = \Phi_S$) to an arbitrary value of η, we obtain

$$\begin{aligned} \Phi - \Phi_S &= -R_d \int_0^\eta T_v d \ln(1-\eta) \\ &\quad -R_d \int_0^\eta T_v d \ln\{\tilde{p}/(1-\eta)\}. \end{aligned} \tag{2.17}$$

Or

$$\Phi - \Phi_S = -R_d \int_0^\eta T_v d \ln \tilde{p}\,. \tag{2.17}'$$

Note that (2.17)′ can also be derived directly using (2.6).

Let us now introduce a generalized geopotential G, defined by

$$\boxed{G \equiv \Phi_S - R_d \int_0^\eta T\, d \ln(1-\eta) + R_d T_0 \Lambda}, \tag{2.18}$$

and a 'virtual' geopotential Φ_v, defined by

$$\boxed{\Phi_v \equiv -R_d \int_0^\eta T_v\, d \ln \tilde{p} + R_d \int_0^\eta T\, d \ln(1-\eta)}. \tag{2.19}$$

Then, using (2.18) and (2.19) in (2.17)′, we obtain

$$\Phi - \Phi_v = -R_d \int_0^{\eta} T \, d\ln(1-\eta) + \Phi_S = G - R_d T_0 \Lambda . \quad (2.20)$$

Or

$$\Phi = G - R_d T_0 \Lambda + \Phi_v . \quad (2.20)'$$

Lastly, the *moisture continuity equation* (2.5) without the source/sink term is recalled

$$\boxed{d_t q = 0}. \quad (2.21)$$

c. Basics of the FISL/SISL scheme

For an arbitrary prognostic variable Ψ (= u, v, $T - \kappa_d T_0 \Lambda$, q, or Λ), each of the prognostic equations (2.15a, 2.15b, 2.14, 2.21, and 2.12) can be expressed as

$$d_t \Psi = F(\Psi) . \quad (2.22)$$

Let us now discretize (2.22) in space and time, along a three-dimensional (3D) backward trajectory. Then, a two time-level, *fully-implicit, semi-Lagrangian* (FISL) scheme for (2.22) can be written as

$$\frac{\Psi^n - \Psi_*^{n-1}}{\Delta t} = \tfrac{1}{2}[(1+\varepsilon_g)F^n + (1-\varepsilon_g)F_*^{n-1}], \quad (2.23)$$

where the superscripts n and n-1 denote the two time levels, Δt denotes the time step, and $\varepsilon_g \in [0,1]$ denotes the un-centering parameter. A dependent variable at time level n-1, with a subscript * is evaluated at the *departure* point (identified here by the asterisk character '*') through a 3D spatial interpolation of the same variable at time level n-1 carried at the grid points. Needless to say, determination of the departure points also involves spatial interpolation. In (2.23), the dependent variables at time level n and without subscripts are carried at the *arrival* grid points.

Introducing the new variables

$$\tau \equiv \tfrac{1}{2}(1+\varepsilon_g)\Delta t , \quad (2.24a)$$

$$R \equiv \frac{\Psi}{\tau} + \frac{1-\varepsilon_g}{1+\varepsilon_g} F , \quad (2.24b)$$

we can rewrite (2.23) as

$$\frac{\Psi^n}{\tau} - F^n = \frac{\Psi_*^{n-1}}{\tau} + \frac{1-\varepsilon_g}{1+\varepsilon_g} F_*^{n-1} = R_*^{n-1} . \quad (2.23)'$$

Then, for the semi-implicit/fully-implicit 'linearization' of (2.23)′, we express F^n as

$$F^n = L^n + N^n , \quad (2.25)$$

where a suitable reference state is assumed and (L, N) denote the *linear* and *nonlinear* parts of F. Using (2.25), we can rewrite (2.23)′ as

$$\frac{\Psi^n}{\tau} - L^n = R_*^{n-1} + N^n \equiv S . \quad (2.26)$$

Notice how (2.26) represents an implicit equation that can be solved iteratively for the unknown variable Ψ^n. To this end, equation (2.26) can be expressed as

$$\left[\frac{\Psi^n}{\tau} - L^n\right]^{(i)} = R_*^{n-1} + \left[N^n\right]^{(i-1)} \equiv S^{(i-1)} , \quad (2.27)$$

where the superscript i denotes an iterative index.

For the *semi-implicit semi-Lagrangian* (SISL) scheme, the nonlinear term N^n in (2.26) is defined *explicitly* using the linear extrapolation in time:

$$N^n \equiv 2N^{n-1} - N^{n-2} . \quad (2.28)$$

Thus, (2.26) together with (2.28) constitute the SISL scheme for (2.22). Clearly, the SISL scheme, unlike the FISL scheme (2.27), does not require any iteration.

As indicated earlier, the FISL scheme proposed here employs 2D semi-Lagrangian horizontal advection. Thus, to be consistent with the FISL scheme, we would consider the SISL scheme that is specifically a 2D SISL scheme. In this context, an equivalent form of (2.22) is derived, where the 3D material time-derivative $d_t \Psi$ is written in terms of the 2D material time-derivative $d_{tH} \Psi$ as

$$d_t \Psi = d_{tH} \Psi + \dot{\eta} \partial_\eta \Psi , \quad (2.29a)$$

where

$$d_{tH} \Psi \equiv \partial_t \Psi + mu \partial_x \Psi + mv \partial_y \Psi , \quad (2.29b)$$

so that (2.22) is reduced to

$$d_{tH} \Psi = F(\Psi) - \dot{\eta} \partial_\eta \Psi \equiv \widetilde{F}(\Psi) . \quad (2.30)$$

The derivations of the FISL/SISL schemes presented earlier for (2.22) holds for (2.30) as well, provided we formally replace F by $\widetilde{F}$, as defined by (2.30), in equations (2.23), (2.24b), and (2.25); also, we need to formally replace N in equations (2.25), (2.26), (2.27), and (2.28) by $\widetilde{N}$, defined by

$$\widetilde{N}(\Psi) \equiv N(\Psi) - \dot{\eta} \partial_\eta \Psi . \quad (2.31)$$

d. Implementation of the FISL/SISL scheme

Let us now apply the semi-Lagrangian schemes described above to the prognostic

equations (2.15a), (2.15b), (2.14), (2.12), and (2.21) for u, v, $T-\kappa_d T_0\Lambda$, Λ, and q, respectively. Thus, using the formal analogy between (2.15a) and (2.22), an analog of (2.23)′ for the *u-momentum equation* (2.15a) is obtained as

$$\frac{u^n}{\tau}-F_u^n=(R_u)_*^{n-1}, \tag{2.32}$$

where

$$R_u\equiv\frac{u}{\tau}+\frac{1-\varepsilon_g}{1+\varepsilon_g}F_u, \tag{2.33}$$

where F_u is defined by (2.15a). Then, using (2.20)′, we can rewrite and *linearize* F_u^n as

$$F_u^n=\left[f_0+(f_z^n-f_0)\right]v^n - m\left[R_d T_v^n\partial_x\ln\widetilde{p}^n+\partial_x(G^n-R_d T_0\Lambda^n+\Phi_v^n)\right].$$

Or

$$F_u^n=(f_0 v^n-m\partial_x G^n)+N_u^n, \tag{2.34}$$

where f_0 is an area-averaged value of f and

$$N_u\equiv(f_z-f_0)v - m[R_d(T_v\partial_x\ln\widetilde{p}-T_0\partial_x\Lambda)+\partial_x\Phi_v]. \tag{2.35}$$

Then, using the formal analogy between (2.34) and (2.25), an analog (2.26) for the *u-momentum equation* is obtained as

$$\boxed{\frac{u^n}{\tau}-f_0 v^n+m\partial_x G^n=N_u^n+(R_u)_*^{n-1}\equiv S_u}. \tag{2.36}$$

Similarly, an analog of (2.26) for the *v-momentum equation* (2.15b) is obtained as

$$\boxed{\frac{v^n}{\tau}+f_0 u^n+m\partial_y G^n=N_v^n+(R_v)_*^{n-1}\equiv S_v}, \tag{2.37}$$

where

$$R_v\equiv\frac{v}{\tau}+\frac{1-\varepsilon_g}{1+\varepsilon_g}F_v, \tag{2.38a}$$

$$N_v\equiv-(f_z-f_0)u - m[R_d(T_v\partial_y\ln\widetilde{p}-T_0\partial_y\Lambda)+\partial_y\Phi_v]. \tag{2.38b}$$

Let us now consider the *thermodynamic energy equation* (2.14). As before, using the formal analogy between (2.14) and (2.22), an analog of (2.23)′ for the *thermodynamic energy equation* is obtained as

$$\frac{\widetilde{T}^n}{\tau}-F_T^n=(R_T)_*^{n-1}, \tag{2.39}$$

where

$$\widetilde{T}\equiv T-\kappa_d T_0\Lambda, \tag{2.40a}$$

$$R_T\equiv\frac{\widetilde{T}}{\tau}+\frac{1-\varepsilon_g}{1+\varepsilon_g}F_T, \tag{2.40b}$$

where F_T is defined by (2.14). Then, using (2.14) and (2.12), we can rewrite and linearize F_T^n as

$$F_T^n=-\kappa_d T_0\frac{\dot{\eta}^n}{1-\eta}+N_T^n, \tag{2.41a}$$

where

$$N_T\equiv \kappa_d\left[\frac{T_v}{1+(\delta-1)q}\left(1-\frac{p_T}{\widetilde{p}}\right)-T_0\right]\left(F_\Lambda-\frac{\dot{\eta}}{1-\eta}\right). \tag{2.41b}$$

Then, using the formal analogy between (2.41a) and (2.25), an analog of (2.26) for the *thermodynamic energy equation* is obtained as

$$\boxed{\frac{\widetilde{T}^n}{\tau}+\kappa_d T_0\frac{\dot{\eta}^n}{1-\eta}=N_T^n+(R_T)_*^{n-1}\equiv S_T}. \tag{2.42}$$

Let us now consider the *mass-continuity equation* (2.12). As before, using the formal analogy between (2.12) and (2.22), an analog (2.23)′ for the mass-continuity equation is obtained as

$$\boxed{\frac{\Lambda^n}{\tau}+\left(D+\partial_\eta\dot{\eta}\right)^n=(R_\Lambda)_*^{n-1}}, \tag{2.43}$$

where

$$R_\Lambda\equiv\frac{\Lambda}{\tau}+\frac{1-\varepsilon_g}{1+\varepsilon_g}F_\Lambda. \tag{2.44}$$

Notice that F_Λ defined by (2.12) is already in a linear form, so that there is no need to derive an analog of (2.26) in this case.

Lastly, we consider the *moisture-continuity equation* (2.21). Using the formal analogy between (2.22) and (2.21), the latter with $F_q\equiv 0$, an analog of (2.23)′ is readily obtained as

$$\boxed{q^n=q_*^{n-1}}. \tag{2.45}$$

As mentioned before, the FISL/SISL schemes proposed here employs 2D semi-Lagrangian horizontal advection. In this case, the moisture continuity equation (2.21), in view of (2.30), is first rewritten as

$$d_{tH}q=-\dot{\eta}\partial_\eta q\equiv\widetilde{F}_q. \tag{2.46a}$$

Then, an analog of (2.23)′ is obtained as

$$\frac{q^n}{\tau}-\widetilde{F}_q^n=(R_q)_*^{n-1}, \tag{2.46b}$$

where

$$R_q\equiv\frac{q}{\tau}+\frac{1-\varepsilon_g}{1+\varepsilon_g}\widetilde{F}_q. \tag{2.46c}$$

Since $\widetilde{F}_q$ given by (2.46a) is a nonlinear function, we express $\widetilde{F}_q^n$ simply as

$$\widetilde{F}_q^n = [zero\ linear\ part] + N_q^n, \qquad (2.46d)$$

where

$$N_q \equiv -\dot{\eta}\partial_\eta q\ . \qquad (2.46e)$$

Then, (2.46b) reduces to the appropriate FISL scheme for the moisture continuity equation (2.21):

$$\boxed{\frac{q^n}{\tau} = N_q^n + (R_q)_*^{n-1} \equiv S_q}. \qquad (2.46f)$$

When 2D semi-Lagrangian horizontal advection is used for the derivations of the FISL/SISL schemes for the prognostic equations for u, v, and $T - \kappa_d T_0 \Lambda$, the functions F_u, F_v, and F_T defined by (2.15a), (2.15b), and (2.14), respectively, are modified into

$$\widetilde{F}_u \equiv F_u - \dot{\eta}\partial_\eta u\ , \qquad (2.47a)$$

$$\widetilde{F}_v \equiv F_v - \dot{\eta}\partial_\eta v\ , \qquad (2.47b)$$

$$\widetilde{F}_T \equiv F_T - \dot{\eta}\partial_\eta T\ . \qquad (2.47c)$$

Clearly, no such modifications are imposed on F_Λ defined by (2.12), as $\partial_\eta \Lambda = 0$. Note that the functions ($\widetilde{F}_u$, $\widetilde{F}_v$, $\widetilde{F}_T$), in turn, will modify the functions (R_u, R_v, R_T) defined by (2.33), (2.38a), and (2.40b), respectively.

Similarly, the functions N_u, N_v, and N_T defined by (2.35), (2.38b), and (2.41b), respectively, are modified into

$$\widetilde{N}_u \equiv N_u - \dot{\eta}\partial_\eta u\ , \qquad (2.47d)$$

$$\widetilde{N}_v \equiv N_v - \dot{\eta}\partial_\eta v\ , \qquad (2.47e)$$

$$\widetilde{N}_T \equiv N_T - \dot{\eta}\partial_\eta T\ . \qquad (2.47f)$$

Note that the functions ($\widetilde{N}_u, \widetilde{N}_v, \widetilde{N}_T$), in turn, will modify the functions (S_u, S_v, S_T) defined by (2.36), (2.37), and (2.42), respectively.

e. Vertical grid and discretization

In this section, we discretize the governing equations, cast already into the form of the FISL/SISL scheme in section 2.d, in the vertical assuming a staggered Lorenz grid with the placement of variables as shown in Fig. 1. We assume there are *K* (integer-) levels between the earth surface ($\widetilde{p} = \widetilde{p}_S$) and the model top ($\widetilde{p} = p_T$). The levels are specified by a sequence of η values, $\{\eta_k\}$ with $1 \le k \le K$, which satisfy $0 < \eta_k < 1$. Each level is bounded by two interfaces, so that there are *K*+1 interfaces (half-integer levels), including the earth surface and the model top. The sequence of interfaces is then denoted by $\{\eta_{k+1/2}\}$ with $0 \le k \le K$, which satisfy $0 \le \eta_{k+1/2} \le 1$. Having specified the model levels, the interfaces are placed at

$$\eta_{k+1/2} = \tfrac{1}{2}(\eta_{k+1} + \eta_k) \quad \forall \quad 1 \le k \le K-1\ , \qquad (2.48a)$$

$$\eta_{1/2} = 0.; \quad \eta_{K+1/2} = 1. \qquad (2.48b)$$

We recognize that a model *layer*, that embeds a model level, is confined between two consecutive interfaces. Then, the thickness of each layer is defined as

$$(\Delta\eta)_k \equiv \eta_{k+1/2} - \eta_{k-1/2} \quad \forall \quad 1 \le k \le K\ . \qquad (2.48c)$$

Similarly, the vertical grid interval between consecutive model levels is defined as

$$(\Delta\eta)_{k+1/2} \equiv \eta_{k+1} - \eta_k \quad \forall \quad 1 \le k \le K-1. \qquad (2.48d)$$

In general, the thickness of each model layer given by (2.48c) is not uniform in η. For later use, we introduce the η-level variable, $\widetilde{\eta}_k$, defined by

$$\widetilde{\eta}_k \equiv \tfrac{1}{2}(\eta_{k+1/2} + \eta_{k-1/2}) \quad \forall \quad 1 \le k \le K\ . \qquad (2.48e)$$

Note that, in general, $\widetilde{\eta}_k \ne \eta_k$.

Having specified the model levels, $\eta_k\ \forall 1 \le k \le K$, we use (2.11a) to determine $\widetilde{p}$ at model levels as

$$\widetilde{p}_k = p_T + (1 - \eta_k)\Pi\ . \qquad (2.48f)$$

For later use in the thermodynamic energy equation, we define the η-coordinate vertical velocity at the levels as

$$\dot{\eta}_k \equiv \tfrac{1}{2}(\dot{\eta}_{k+1/2} + \dot{\eta}_{k-1/2}) \quad \forall \quad 1 \le k \le K\ , \qquad (2.48g)$$

where

$$\dot{\eta}_{1/2} = 0 = \dot{\eta}_{K+1/2}\ , \qquad (2.48h)$$

that corresponds to (2.9). Similarly, for later use in the hydrostatic equation, we define the virtual temperature at the model interfaces (excluding the model top) as

$$(T_v)_{k+1/2} = \tfrac{1}{2}\left[(T_v)_{k+1} + (T_v)_k\right] \forall\ 1 \le k \le K-1\ , \qquad (2.48i)$$

$$(T_v)_{1/2} = \tfrac{1}{2}\left[(T_v)_1 + (T_v)_1\right] = (T_v)_1\ . \qquad (2.48j)$$

- *Hydrostatic equation*

Let us apply (2.6) at the interfaces $k+1/2 \ \forall\ 0 \le k \le K-1$, to obtain

$$\Phi_{k+1} - \Phi_k = -R_d (T_v)_{k+1/2} (\ln \widetilde{p}_{k+1} - \ln \widetilde{p}_k), \quad 1 \le k \le K-1 \tag{2.49a}$$

$$\Phi_1 - \Phi_S = -R_d (T_v)_{1/2} (\ln \widetilde{p}_1 - \ln \widetilde{p}_S), \tag{2.49b}$$

where $(T_v)_{k+1/2} \ \forall\ 0 \le k \le K-1$, are given by (2.48i) and (2.48j).

Let us now rewrite the $\ln \widetilde{p}_k$ terms of (2.49a) and (2.49b), in view of (2.16), as follows. Using (2.48f), we obtain

$$\ln \widetilde{p}_k = \ln(1-\eta_k) + \ln \frac{\widetilde{p}_k}{1-\eta_k}, \quad 1 \le k \le K. \tag{2.49c}$$

Then, $\forall\ 1 \le k \le K-1$

$$\ln \widetilde{p}_{k+1} - \ln \widetilde{p}_k = \{\ln(1-\eta_{k+1}) - \ln(1-\eta_k)\} + \left\{ \ln \frac{\widetilde{p}_{k+1}}{1-\eta_{k+1}} - \ln \frac{\widetilde{p}_k}{1-\eta_k} \right\}$$
$$= \ln \frac{1-\eta_{k+1}}{1-\eta_k} + \ln \left\{ \frac{\widetilde{p}_{k+1}}{\widetilde{p}_k} \frac{1-\eta_k}{1-\eta_{k+1}} \right\}. \tag{2.49d}$$

Also,

$$\ln \widetilde{p}_1 - \ln \widetilde{p}_S = \ln(1-\eta_1) + \ln \left\{ \frac{\widetilde{p}_1}{\widetilde{p}_S} \frac{1}{1-\eta_1} \right\}. \tag{2.49e}$$

To rewrite (2.49d) and (2.49e) in a compact from, let us introduce the 'interface' variables, $\delta_{k+1/2}$ and $\hat{\delta}_{k+1/2} \quad \forall \quad 0 \le k \le K-1$:

$$\delta_{1/2} \equiv \ln(1-\eta_1); \quad \hat{\delta}_{1/2} \equiv \ln \left\{ \frac{\widetilde{p}_1}{\widetilde{p}_S} \frac{1}{1-\eta_1} \right\}, \tag{2.49f}$$

$$\delta_{k+1/2} \equiv \ln \frac{1-\eta_{k+1}}{1-\eta_k}; \hat{\delta}_{k+1/2} \equiv \ln \left\{ \frac{\widetilde{p}_{k+1}}{\widetilde{p}_k} \frac{1-\eta_k}{1-\eta_{k+1}} \right\}, \tag{2.49g}$$

and then rewrite (2.49d) and (2.49e) as

$$\ln \widetilde{p}_{k+1} - \ln \widetilde{p}_k = \delta_{k+1/2} + \hat{\delta}_{k+1/2} \quad \forall \quad 1 \le k \le K-1, \tag{2.49d}′$$

$$\ln \widetilde{p}_1 - \ln \widetilde{p}_S = \delta_{1/2} + \hat{\delta}_{1/2}. \tag{2.49e}′$$

Using (2.49d)′, (2.49e)′, (2.48i), and (2.48j), we can rewrite (2.49a) and (2.49b) as

$$\Phi_{k+1} - \Phi_k = -\tfrac{1}{2} R_d \left[(T_v)_{k+1} + (T_v)_k \right] (\delta_{k+1/2} + \hat{\delta}_{k+1/2}) \tag{2.49a}′$$
$$\forall \quad 1 \le k \le K-1,$$

$$\Phi_1 - \Phi_S = -R_d (T_v)_1 (\delta_{1/2} + \hat{\delta}_{1/2}). \tag{2.49b}′$$

The two equations above constitute a vertically-discrete analog of the continuous-form hydrostatic equation (2.6)′.

Changing the subscript in (2.49a)′ from k to l, and then summing up the equations over $1 \le l \le k-1$, we obtain

$$\sum_{l=1}^{k-1} (\Phi_{l+1} - \Phi_l) = -\tfrac{1}{2} R_d \sum_{l=1}^{k-1} [(T_v)_{l+1} + (T_v)_l] (\delta_{l+1/2} + \hat{\delta}_{l+1/2})$$
$$= -\tfrac{1}{2} R_d [\sum_{l=2}^{k} (T_v)_l (\delta_{l-1/2} + \hat{\delta}_{l-1/2}) + \sum_{l=1}^{k-1} (T_v)_l (\delta_{l+1/2} + \hat{\delta}_{l+1/2})]$$
$$= -\tfrac{1}{2} R_d [(T_v)_k (\delta_{k-1/2} + \hat{\delta}_{k-1/2}) + \sum_{l=2}^{k-1} (T_v)_l (\delta_{l-1/2} + \hat{\delta}_{l-1/2} + \delta_{l+1/2} + \hat{\delta}_{l+1/2}) + (T_v)_1 (\delta_{3/2} + \hat{\delta}_{3/2})].$$

Or

$$\Phi_k - \Phi_1 = -R_d [\tfrac{1}{2} (\delta_{3/2} + \hat{\delta}_{3/2}) (T_v)_1 + \sum_{l=2}^{k-1} \tfrac{1}{2} (\delta_{l-1/2} + \hat{\delta}_{l-1/2} + \delta_{l+1/2} + \hat{\delta}_{l+1/2}) (T_v)_l + \tfrac{1}{2} (\delta_{k-1/2} + \hat{\delta}_{k-1/2}) (T_v)_k]. \tag{2.49h}$$

Then, adding (2.49h) and (2.49b)′, we obtain

$$\Phi_k - \Phi_S = -R_d [\{(\delta_{1/2} + \hat{\delta}_{1/2}) + \tfrac{1}{2} (\delta_{3/2} + \hat{\delta}_{3/2})\} (T_v)_1 + \sum_{l=2}^{k-1} \tfrac{1}{2} (\delta_{l-1/2} + \hat{\delta}_{l-1/2} + \delta_{l+1/2} + \hat{\delta}_{l+1/2}) (T_v)_l + \tfrac{1}{2} (\delta_{k-1/2} + \hat{\delta}_{k-1/2}) (T_v)_k]. \tag{2.49i}$$

Note that (2.49i) holds for $2 \le k \le K$ with the Σ term omitted for $k = 2$. Equation (2.49b)′ holds for $k = 1$.

Equations (2.49i) and (2.49b)′ can be written in a compact form:

$$\Phi_k = \Phi_S - R_d \sum_{l=1}^{k} (a_{k,l} + \hat{a}_{k,l}) (T_v)_l \ \forall\ 1 \le k \le K, \tag{2.49j}$$

that is a vertically-discrete analog of the corresponding continuous-form vertically-integrated hydrostatic equation (2.17) from section 2.b. Here, $a_{k,l}$ and $\hat{a}_{k,l}$ are the elements of the lower triangular matrices $\mathbf{A}$ and $\hat{\mathbf{A}}$ of dimension $K \times K$, the non-zero elements of which are given by

$$a_{1,1} = \delta_{1/2}\,, \tag{2.49k}$$

$$a_{2,1} = \delta_{1/2} + \tfrac{1}{2}\delta_{3/2}; \quad a_{2,2} = \tfrac{1}{2}\delta_{3/2}\,. \tag{2.49l}$$

For $3 \le k \le K$

$$a_{k,l} = \begin{cases} \delta_{1/2} + \frac{1}{2}\delta_{3/2} & \forall \quad l = 1 \\ \frac{1}{2}(\delta_{l-1/2} + \delta_{l+1/2}) & \forall \quad 2 \le l \le k-1 \\ \frac{1}{2}\delta_{l-1/2} & \forall \quad l = k. \end{cases} \tag{2.49m}$$

$$\hat{a}_{1,1} = \hat{\delta}_{1/2}\,, \tag{2.49n}$$

$$\hat{a}_{2,1} = \hat{\delta}_{1/2} + \tfrac{1}{2}\hat{\delta}_{3/2}; \quad \hat{a}_{2,2} = \tfrac{1}{2}\hat{\delta}_{3/2}\,. \tag{2.49o}$$

For $3 \le k \le K$

$$\hat{a}_{k,l} = \begin{cases} \hat{\delta}_{1/2} + \frac{1}{2}\hat{\delta}_{3/2} & \forall \quad l = 1 \\ \frac{1}{2}(\hat{\delta}_{l-1/2} + \hat{\delta}_{l+1/2}) & \forall \quad 2 \le l \le k-1 \\ \frac{1}{2}\hat{\delta}_{l-1/2} & \forall \quad l = k. \end{cases} \tag{2.49p}$$

In view of (2.49f) and (2.49g), we note that elements of the matrix **A** are functions of the η-values, η_k, at the model levels, $1 \le k \le K$. Since the $\{\eta_k\}$ values are specified constants, the matrix **A** does not change in time. However, a similar inspection also reveals that the elements of the matrix $\hat{\mathbf{A}}$ can vary both in space and time. This is not a problem, as the matrix $\hat{\mathbf{A}}$ does not need to be computed explicitly anywhere in subsequent development of the FISL/SISL scheme.

In analogy with (2.18), the generalized geopotential at levels $1 \le k \le K$, is introduced as

$$G_k = \Phi_S - R_d \sum_{l=1}^{k} a_{k,l} T_l + R_d T_0 \Lambda\,. \tag{2.49q}$$

Similarly, in analogy with (2.19), the virtual geopotential at levels $1 \le k \le K$, is introduced as

$$(\Phi_v)_k = -R_d \sum_{l=1}^{k} (a_{k,l} + \hat{a}_{k,l})(T_v)_l + R_d \sum_{l=1}^{k} a_{k,l} T_l\,. \tag{2.49r}$$

Then, adding (2.49q) and (2.49r), we obtain

$$\begin{aligned} G_k + (\Phi_v)_k = \Phi_S & \\ - R_d \sum_{l=1}^{k} (a_{k,l} + \hat{a}_{k,l})(T_v)_l & \\ + R_d T_0 \Lambda = \Phi_k + R_d T_0 \Lambda. & \end{aligned} \tag{2.49s}$$

Or

$$\Phi_k = G_k - R_d T_0 \Lambda + (\Phi_v)_k \;\; \forall \, 1 \le k \le K\,. \tag{2.49t}$$

- *Mass continuity equation*

Let us apply (2.43), (2.44), and (2.12) at levels $1 \le k \le K$, to obtain

$$\frac{\Lambda^n}{\tau} + D_k^n + \frac{\dot{\eta}_{k+1/2}^n - \dot{\eta}_{k-1/2}^n}{(\Delta\eta)_k} = [(R_\Lambda)_k]_*^{n-1}\,, \tag{2.50a}$$

where

$$(R_\Lambda)_k \equiv \frac{\Lambda}{\tau} + \frac{1-\varepsilon_g}{1+\varepsilon_g}(F_\Lambda)_k\,, \tag{2.50b}$$

$$(F_\Lambda)_k \equiv -\left[D_k + \frac{\dot{\eta}_{k+1/2} - \dot{\eta}_{k-1/2}}{(\Delta\eta)_k} \right]. \tag{2.50c}$$

Moreover, let us rewrite (2.50a) as

$$\frac{\Lambda^n}{\tau} + \frac{\dot{\eta}_{k+1/2}^n - \dot{\eta}_{k-1/2}^n}{(\Delta\eta)_k} = X_k\,, \tag{2.50d}$$

where

$$X_k \equiv [(R_\Lambda)_k]_*^{n-1} - D_k^n \quad \forall \quad 1 \le k \le K\,. \tag{2.50e}$$

Then, summing up (2.50d) times $(\Delta\eta)_k$ over all levels $1 \le k \le K$, we obtain

$$\frac{\Lambda^n}{\tau}\sum_{k=1}^{K}(\Delta\eta)_k + \sum_{k=1}^{K}(\dot{\eta}_{k+1/2}^n - \dot{\eta}_{k-1/2}^n) = \sum_{k=1}^{K}(X\Delta\eta)_k\,,$$

or

$$\frac{\Lambda^n}{\tau}(\eta_{K+1/2} - \eta_{1/2}) + (\dot{\eta}_{K+1/2}^n - \dot{\eta}_{1/2}^n) = \sum_{k=1}^{K}(X\Delta\eta)_k\,,$$

or

$$\boxed{\Lambda^n = \tau \sum_{k=1}^{K}(X\Delta\eta)_k}\,. \tag{2.50f}$$

Note that to arrive at (2.50f) from the previous equation, we have used the lower and upper boundary conditions, corresponding to (2.9), on $\dot{\eta}_{k+1/2}^n$ given by

$$\dot{\eta}_{1/2}^n = 0; \quad \dot{\eta}_{K+1/2}^n = 0 \quad \forall \quad \text{all } n\,, \tag{2.50g}$$

and also the relations

$$\eta_{1/2} = 0; \quad \eta_{K+1/2} = 1\,. \tag{2.50h}$$

Similarly, after formally replacing the vertical grid-index k by l in (2.50d), and then summing up (2.50d) times $(\Delta\eta)_l$ over the levels $k \le l \le K$, we obtain

$$\frac{\Lambda^n}{\tau}\sum_{l=k}^{K}(\Delta\eta)_l + \sum_{l=k}^{K}(\dot{\eta}_{l+1/2}^n - \dot{\eta}_{l-1/2}^n) = \sum_{l=k}^{K}(X\Delta\eta)_l\,.$$

Or

$$\frac{\Lambda^n}{\tau}(\eta_{K+1/2} - \eta_{k-1/2}) + (\dot{\eta}_{K+1/2}^n - \dot{\eta}_{k-1/2}^n) = \sum_{l=k}^{K}(X\Delta\eta)_l\,.$$

Or

$$\dot{\eta}_{k-1/2}^n = (1 - \eta_{k-1/2})\frac{\Lambda^n}{\tau} - \sum_{l=k}^{K}(X\Delta\eta)_l\,. \tag{2.50i}$$

Note that in deriving (2.50i) from the previous equation, we have used the second equations from (2.50g) and (2.50h).

Then, using (2.50f) to eliminate Λ^n/τ from (2.50i), we obtain $\dot{\eta}^n$ at the model interfaces, $k-1/2 \quad \forall \quad 2 \le k \le K$:

$$\dot{\eta}^n_{k-1/2} = (1-\eta_{k-1/2}) \sum_{l=1}^{K} (X\Delta\eta)_l - \sum_{l=k}^{K} (X\Delta\eta)_l \ .$$

Or

$$\boxed{\dot{\eta}^n_{k-1/2} = \sum_{l=1}^{k-1} (X\Delta\eta)_l - \eta_{k-1/2} \sum_{l=1}^{K} (X\Delta\eta)_l \ \forall \ \ 2 \le k \le K.} \tag{2.50j}$$

To determine $\dot{\eta}^n$ at the model levels $1 \le k \le K$, we substitute (2.50j) in (2.48g) to obtain

$$\begin{aligned}
\dot{\eta}^n_k &= \tfrac{1}{2}\Big[\sum_{l=1}^{k} (X\Delta\eta)_l + \sum_{l=1}^{k-1} (X\Delta\eta)_l\Big] \\
&\quad - \tfrac{1}{2}(\eta_{k+1/2} + \eta_{k-1/2}) \sum_{l=1}^{K} (X\Delta\eta)_l \\
&= \tfrac{1}{2}\Big[(X\Delta\eta)_k + 2\sum_{l=1}^{k-1} (X\Delta\eta)_l\Big] - \tilde{\eta}_k \sum_{l=1}^{K} (X\Delta\eta)_l \\
&= \Big[\sum_{l=1}^{k-1} (X\Delta\eta)_l + \tfrac{1}{2}(X\Delta\eta)_k\Big] - \tilde{\eta}_k \sum_{l=1}^{K} (X\Delta\eta)_l \ ,
\end{aligned} \tag{2.50k}$$

where (2.48e) has been used.

Let us introduce a discrete vertical integral operator, Σ', as

$$\sum_{l=1}^{k}{}' \Psi_l = \sum_{l=1}^{k-1} \Psi_l + \tfrac{1}{2}\Psi_k \,, \tag{2.50l}$$

so that (2.50k) can be rewritten as

$$\boxed{\dot{\eta}^n_k = \sum_{l=1}^{k}{}' (X\Delta\eta)_l - \tilde{\eta}_k \sum_{l=1}^{K} (X\Delta\eta)_l \ \forall \ 1 \le k \le K}. \tag{2.50m}$$

- *Thermodynamic energy equation*

Let us apply (2.42) at model levels $1 \le k \le K$, to obtain

$$\frac{\tilde{T}^n_k}{\tau} + \kappa_d T_0 \frac{\dot{\eta}^n_k}{1-\eta_k} = (S_T)_k \,, \tag{2.51a}$$

where

$$\tilde{T}_k \equiv T_k - \kappa_d T_0 \Lambda \,, \tag{2.51b}$$

$$(S_T)_k = (N_T)^n_k + [(R_T)_k]^{n-1}_* \,, \tag{2.51c}$$

$$(R_T)_k = \frac{\tilde{T}_k}{\tau} + \frac{1-\varepsilon_g}{1+\varepsilon_g}(F_T)_k \,, \tag{2.51d}$$

$$\begin{aligned}
(F_T)_k &= \kappa_d \frac{(T_v)_k}{1+(\delta-1)q_k}\left(1 - \frac{p_T}{\tilde{p}_k}\right) \\
&\quad \times\left\{(F_\Lambda)_k - \frac{\dot{\eta}_k}{1-\eta_k}\right\} - \kappa_d T_0 (F_\Lambda)_k \,,
\end{aligned} \tag{2.51e}$$

$$\begin{aligned}
(N_T)_k &= \kappa_d \left[\frac{(T_v)_k}{1+(\delta-1)q_k}\left(1 - \frac{p_T}{\tilde{p}_k}\right) - T_0\right] \\
&\quad \times\left\{(F_\Lambda)_k - \frac{\dot{\eta}_k}{1-\eta_k}\right\},
\end{aligned} \tag{2.51f}$$

where $(F_\Lambda)_k$ is given by (2.50c).

Eliminating Λ^n and $\dot{\eta}^n_k$ from (2.51a), using (2.50f) and (2.50m), respectively, we obtain

$$\begin{aligned}
T^n_k &= \tau\left[(S_T)_k - \kappa_d T_0 \frac{\dot{\eta}^n_k}{1-\eta_k}\right] + \kappa_d T_0 \Lambda^n \\
&= \tau\left[(S_T)_k - \frac{\kappa_d T_0}{1-\eta_k}\left\{\sum_{l=1}^{k}{}' (X\Delta\eta)_l - \tilde{\eta}_k \sum_{l=1}^{K} (X\Delta\eta)_l\right\}\right] + \kappa_d T_0 \tau \sum_{l=1}^{K} (X\Delta\eta)_l \\
&= \tau\left[(S_T)_k - \frac{\kappa_d T_0}{1-\eta_k}\sum_{l=1}^{k}{}' (X\Delta\eta)_l + \kappa_d T_0\left(1 + \frac{\tilde{\eta}_k}{1-\eta_k}\right)\sum_{l=1}^{K} (X\Delta\eta)_l\right]
\end{aligned}$$

Or

$$T^n_k = \tau\left[(S_T)_k - \frac{\kappa_d T_0}{1-\eta_k}\left\{\sum_{l=1}^{k}{}' (X\Delta\eta)_l + (-1+\eta_k - \tilde{\eta}_k)\sum_{l=1}^{K} (X\Delta\eta)_l\right\}\right] \tag{2.51g}$$

- *Momentum equations*

Let us apply (2.36) and (2.37) at model levels $1 \le k \le K$, to obtain

$$\frac{u^n_k}{\tau} - f_0 v^n_k + m\partial_x G^n_k = (S_u)_k \,, \tag{2.52a}$$

$$\frac{v^n_k}{\tau} + f_0 u^n_k + m\partial_y G^n_k = (S_v)_k \,, \tag{2.52b}$$

where

$$\begin{aligned}
(S_u)_k &= (N_u)^n_k + [(R_u)_k]^{n-1}_* ; \\
(S_v)_k &= (N_v)^n_k + [(R_v)_k]^{n-1}_*
\end{aligned} \,, \tag{2.52c}$$

$$(R_u)_k = \frac{u_k}{\tau} + \frac{1-\varepsilon_g}{1+\varepsilon_g}(F_u)_k ; \ (R_v)_k = \frac{v_k}{\tau} + \frac{1-\varepsilon_g}{1+\varepsilon_g}(F_v)_k \,, \tag{2.52d}$$

$$\begin{aligned}
(N_u)_k &= [(f_z)_k - f_0]v_k \\
&\quad - m[R_d\left\{(T_v)_k \partial_x \ln \tilde{p}_k - T_0 \partial_x \Lambda\right\} \\
&\quad + \partial_x (\Phi_v)_k],
\end{aligned} \tag{2.52e}$$

$$(N_v)_k = -[(f_z)_k - f_0]u_k - m[R_d\{(T_v)_k \partial_y \ln \tilde{p}_k - T_0 \partial_y \Lambda\}, \quad (2.52f)$$
$$+\partial_y(\Phi_v)_k],$$

$$(F_u)_k = (f_z v)_k - m\{R_d (T_v)_k \partial_x \ln \tilde{p}_k + \partial_x \Phi_k\}, \quad (2.52g)$$

$$(F_v)_k = -(f_z u)_k - m\{R_d (T_v)_k \partial_y \ln \tilde{p}_k + \partial_y \Phi_k\}. \quad (2.52h)$$

Then, from (2.52a) and (2.52b), we obtain

$$u_k^n = \hat{\tau}[(H_u)_k - m(\partial_x G_k^n + f_0 \tau \partial_y G_k^n)], \quad (2.52i)$$

$$v_k^n = \hat{\tau}[(H_v)_k - m(\partial_y G_k^n - f_0 \tau \partial_x G_k^n)], \quad (2.52j)$$

where

$$\hat{\tau} \equiv \tau / [1 + (f_0 \tau)^2], \quad (2.52k)$$

$$(H_u)_k = (S_u)_k + f_0 \tau (S_v)_k; \quad (H_v)_k = (S_v)_k - f_0 \tau (S_u)_k. \quad (2.52l)$$

From (2.52i) and (2.52j), we derive the horizontal divergence at the model levels $1 \le k \le K$,

$$D_k^n = m^2[\partial_x(u_k^n / m) + \partial_y(v_k^n / m)]$$
$$= \hat{\tau} m^2[\partial_x\{(H_u)_k / m\} + \partial_y\{(H_v)_k / m\} - (\partial_{xx} + \partial_{yy}) G_k^n].$$

Or

$$\boxed{D_k^n + \hat{\tau} \nabla_H^2 G_k^n = P_k \quad \forall \quad 1 \le k \le K}, \quad (2.52m)$$

where

$$\nabla_H^2 \Psi_k \equiv m^2(\partial_{xx} + \partial_{yy})\Psi, \quad (2.52n)$$

$$P_k \equiv \hat{\tau} m^2[\partial_x\{(H_u)_k / m\} + \partial_y\{(H_v)_k / m\}]. \quad (2.52o)$$

- *Moisture continuity equation*

For 3D semi-Lagrangian advection based FISL/SISL schemes, we apply (2.45) at the model levels $1 \le k \le K$, to obtain

$$q_k^n = (q_k)_*^{n-1}. \quad (2.53a)$$

For 2D semi-Lagrangian advection based FISL/SISL schemes, we apply (2.46f) at model levels $1 \le k \le K$, to obtain

$$\frac{q_k^n}{\tau} = (S_q)_k, \quad (2.53b)$$

where

$$(S_q)_k = (N_q)_k^n + [(R_q)_k]_*^{n-1}, \quad (2.53c)$$

$$(R_q)_k = \frac{q_k}{\tau} + \frac{1 - \varepsilon_g}{1 + \varepsilon_g}(\tilde{F}_q)_k, \quad (2.53d)$$

$$(\tilde{F}_q)_k = (N_q)_k, \quad (2.53e)$$

$$(N_q)_k = -(\dot{\eta}\partial_\eta q)_k. \quad (2.53f)$$

Note that for the vertical advection of an arbitrary variable, Ψ:

$$(\dot{\eta}\partial_\eta \Psi)_k = \tfrac{1}{2}\left[\dot{\eta}_{k+1/2} \frac{\Psi_{k+1} - \Psi_k}{(\Delta\eta)_{k+1/2}} + \dot{\eta}_{k-1/2} \frac{\Psi_k - \Psi_{k-1}}{(\Delta\eta)_{k-1/2}}\right] \quad \forall \quad 1 \le k \le K. \quad (2.53g)$$

- *Elliptic equations*

In this section, we use the vertically discrete equations established thus far, to derive a vertically-decoupled system of 2D elliptic equations for the generalized geopotential G^n. To start, we apply (2.49q) at the time level n, to obtain

$$G_k^n = \Phi_S + R_d T_0 \Lambda^n - R_d \sum_{l=1}^{k} a_{k,l} T_l^n, \quad (2.54a)$$

where $1 \le k \le K$. Then, eliminating Λ^n and T_l^n from (2.54a), using (2.50f) and (2.51g), respectively, we obtain

$$G_k^n = \Phi_S + R_d T_0 \tau \sum_{l=1}^{K} (X\Delta\eta)_l - R_d \tau \sum_{m=1}^{k} a_{k,m}\left[(S_T)_m - \frac{\kappa_d T_0}{1 - \eta_m}\left\{\sum_{l=1}^{m}{}' (X\Delta\eta)_l + (-1 + \eta_m - \tilde{\eta}_m)\sum_{l=1}^{K}(X\Delta\eta)_l\right\}\right]$$

Or

$$G_k^n = \Phi_S - \tau R_d \sum_{m=1}^{k} a_{k,m}(S_T)_m + \tau R_d T_0 \sum_{l=1}^{K} (X\Delta\eta)_l + \tau R_d \kappa_d T_0 \underline{\sum_{m=1}^{k} \frac{a_{k,m}}{1 - \eta_m}\left\{\sum_{l=1}^{m}{}' (X\Delta\eta)_l + (-1 + \eta_m - \tilde{\eta}_m)\sum_{l=1}^{K}(X\Delta\eta)_l\right\}} \quad (2.54b)$$

Note that the subscript m used in (2.54a) and (2.54b), and in the equations derived later based on these two equations, should not be confused with the map factor also denoted by m.

Let us denote the underlined term in (2.54b) by Y_k and then using (2.50l) express it as

$$Y_k = \sum_{m=1}^{k} \frac{a_{k,m}}{1 - \eta_m}\{(\underline{-1 + \eta_m} - \tilde{\eta}_m)\sum_{l=1}^{m-1}(X\Delta\eta)_l + (\tfrac{1}{2}\underline{-1 + \eta_m} - \tilde{\eta}_m)(X\Delta\eta)_m + (\underline{-1 + \eta_m} - \tilde{\eta}_m)\sum_{l=m+1}^{K}(X\Delta\eta)_l\}. \quad (2.54c)$$

Let us then introduce the matrix $\mathbf{J} = [J_{m,l}]_{K \times K}$:

$$J_{m,l} = \begin{cases} 0 & \forall \quad l < m \\ \frac{1}{2} & \forall \quad l = m \\ 1 & \forall \quad l > m \end{cases}, \quad (2.54d)$$

so that

$$1 - J_{m,l} = \begin{cases} 1 & \forall \quad l < m \\ \frac{1}{2} & \forall \quad l = m \\ 0 & \forall \quad l > m. \end{cases} \qquad (2.54e)$$

Then, using (2.54e), we can rewrite (2.54c) as

$$Y_k = \sum_{m=1}^{k} \frac{a_{k,m}}{1-\eta_m} \sum_{l=1}^{K} (1 - J_{m,l} \underline{-1 + \eta_m} - \tilde{\eta}_m)(X\Delta\eta)_l$$

$$= \sum_{l=1}^{K} [\sum_{m=1}^{k} \frac{a_{k,m}}{1-\eta_m} \{1 - J_{m,l} + (\underline{-1 + \eta_m} - \tilde{\eta}_m)\}](X\Delta\eta)_l \qquad (2.54f)$$

Substituting Y_k from (2.54f) into (2.54b), we obtain

$$G_k^n = \Phi_S - \tau R_d \sum_{m=1}^{k} a_{k,m} (S_T)_m + \tau R_d T_0 \sum_{l=1}^{K} [1 + \kappa_d \sum_{m=1}^{k} \frac{a_{k,m}}{1-\eta_m} \{1 - J_{m,l} + (-1 + \eta_m - \tilde{\eta}_m)\}](X\Delta\eta)_l \qquad (2.54g)$$

Let us introduce the matrix $\mathbf{M} \equiv [M_{k,l}]_{K \times K}$:

$$M_{k,l} = R_d T_0 (\Delta\eta)_l \left[1 + \kappa_d \sum_{m=1}^{k} \frac{a_{k,m}}{1-\eta_m} \{1 - J_{m,l} + (-1 + \eta_m - \tilde{\eta}_m)\} \right] \qquad (2.54h)$$

and employ (2.50e), to rewrite (2.54g) as

$$G_k^n = \Phi_S - \tau R_d \sum_{m=1}^{k} a_{k,m} (S_T)_m + \tau \sum_{l=1}^{K} M_{k,l} \{[(R_\Lambda)_l]_*^{n-1} - D_l^n\}$$

Or

$$\boxed{G_k^n + \tau \sum_{l=1}^{K} M_{k,l} D_l^n = H_k \quad \forall \quad 1 \le k \le K}, \qquad (2.54i)$$

where

$$H_k = \Phi_S - \tau R_d \sum_{m=1}^{k} a_{k,m} (S_T)_m + \tau \sum_{l=1}^{K} M_{k,l} [(R_\Lambda)_l]_*^{n-1}. \qquad (2.54j)$$

Let us now introduce the K-dimensional column-vectors (**D**, **G**, **P**, **H**) whose respective elements are (D_k^n, G_k^n, P_k, H_k). Then, (2.54i) and (2.52m) can be expressed in matrix form:

$$\mathbf{G} + \tau \mathbf{M} \mathbf{D} = \mathbf{H}, \qquad (2.54k)$$

$$\mathbf{D} + \hat{\tau} \nabla_H^2 \mathbf{G} = \mathbf{P}. \qquad (2.54l)$$

A vertical decoupling transformation is also introduced at this stage. Let **E** be the $K \times K$ matrix whose column vectors are the eigen vectors of **M**, with the associated eigen values (K in number) λ_1, λ_2, …, λ_K. Multiplying (2.54k) and (2.54l) on the left by the matrix $\mathbf{E}^{-1}$, we obtain

$$\hat{\mathbf{G}} + \tau (\lambda_k \delta_{k,l}) \hat{\mathbf{D}} = \hat{\mathbf{H}}, \qquad (2.54m)$$

$$\hat{\mathbf{D}} + \hat{\tau} \nabla_H^2 \hat{\mathbf{G}} = \hat{\mathbf{P}}, \qquad (2.54n)$$

where

$$(\hat{\mathbf{D}}, \hat{\mathbf{G}}, \hat{\mathbf{P}}, \hat{\mathbf{H}}) = \mathbf{E}^{-1} (\mathbf{D}, \mathbf{G}, \mathbf{P}, \mathbf{H}), \qquad (2.54o)$$

and $(\lambda_k \delta_{k,l})$ is a diagonal matrix; $\delta_{k,l}$ is the Kronecker delta.

Resorting to the component form, (2.54m) and (2.54n) can be written as

$$\hat{G}_k + \tau \lambda_k \hat{D}_k = \hat{H}_k, \qquad (2.54p)$$

$$\hat{D}_k + \hat{\tau} \nabla_H^2 \hat{G}_k = \hat{P}_k, \qquad (2.54q)$$

where $(\hat{D}_k, \hat{G}_k, \hat{P}_k, \hat{H}_k)$ are the elements of the respective vectors $(\hat{\mathbf{D}}, \hat{\mathbf{G}}, \hat{\mathbf{P}}, \hat{\mathbf{H}})$ defined by (2.54o).

Eliminating $\hat{D}_k$ from (2.54p) and (2.54q), we obtain a set of 2D Helmholtz-type elliptic equations for the vertical eigen modes (K in number):

$$\hat{G}_k + \tau \lambda_k [\hat{P}_k - \hat{\tau} \nabla_H^2 \hat{G}_k] = \hat{H}_k.$$

Or

$$\hat{\tau} \nabla_H^2 \hat{G}_k - \frac{1}{\tau \lambda_k} \hat{G}_k = \hat{P}_k - \frac{\hat{H}_k}{\tau \lambda_k}.$$

Or

$$\boxed{\frac{1}{1 + (f_0 \tau)^2} \nabla_H^2 \hat{G}_k - \frac{1}{\tau^2 \lambda_k} \hat{G}_k = \frac{\hat{P}_k}{\tau} - \frac{\hat{H}_k}{\tau^2 \lambda_k} \equiv \Im_k \quad \forall \quad 1 \le k \le K.} \qquad (2.54r)$$

Note the elliptic equation (2.54r) is non-separable, because of the non-separable map-factor term $m(x, y)$ that appears inside the $\nabla_H^2 \hat{G}_k$ term defined by (2.52n).

For $T_0 = 300\,K$, and number of model levels, $K = 10$, we have computed the eigen-values $\{\lambda_k\}\ \forall\ 1 \le k \le K$ and the eigen-vectors of the matrix **M**. For simplicity, the model layers are assumed of uniform thickness in η, so that $(\Delta\eta)_k = 1/K\ \forall\ 1 \le k \le K$; and the model levels are placed at $\eta_k = \frac{1}{2}(\eta_{k+1/2} + \eta_{k-1/2})\ \forall\ 1 \le k \le K$. The pure gravity wave speed associated with the k^{th} eigen-mode is given by $(c_g)_k = \sqrt{\lambda_k}$ for $1 \le k \le K$. Figure 2 shows $(c_g)_k$ as a function of the eigen-mode number k. Here the eigen-values are arranged in a descending order in terms of the gravity-wave speed. The corresponding eigen-vectors are normalized by

making the 1st element of each vector positive; and then dividing each element of the vector by the largest element of that vector in terms of absolute value. The normalized eigen-vectors for the eigen-modes 1-5 are shown in Fig. 3a, and for the eigen-modes 6-10 are shown in Fig. 3b. The eigen-modes 1, 2, 3, …, are identified as the external (or Lamb) mode, the 1st internal mode, the 2nd internal mode, …, respectively. Since the external mode is the fastest, a gravity-wave Courant number can be introduced for the model as

$$\mu_g \equiv (c_g)_1 \Delta t / \Delta \,, \qquad (2.54s)$$

where Δ is assumed to be the uniform grid size in x and y. Clearly for any 2nd order time-explicit scheme to be linearly stable, it must satisfy the CFL restriction:

$$\mu_{ex} \equiv [(c_g)_1 (\Delta t)_{ex} / \Delta] \le 1/2 \,, \qquad (2.54t)$$

where the subscript *ex* is a reminder for the time-explicit scheme.

f. Horizontal grid and discretization

As indicated in the Introduction, the unstaggered A grid with a uniform grid interval Δ in x and y is used to horizontally discretize the governing equations. Standard second-order centered-difference scheme is used to discretize all partial derivative terms in x and y. The Laplacian operator defined by (2.52n) is discretized horizontally as

$$(\nabla_H^2 \Psi)_{i,j} = \frac{m_{i,j}^2}{\Delta^2}(\Psi_{i+1,j} + \Psi_{i-1,j} + \Psi_{i,j+1} + \Psi_{i,j-1} - 4\Psi_{i,j}) \quad \forall \quad (i,j) \in L_D \qquad (2.54u)$$

using a compact stencil of five grid points, where the neighboring points are one grid interval apart. The limited-area horizontal domain used for the model is shown in Fig. 4. The scheme (2.54u) has been employed in the Helmholtz-type equation (2.54r) to eliminate the spurious two-grid-interval gravity wave solutions that may appear as noisy checkerboard patterns in the model forecasts. Use of such a compact stencil enables a gravity-wave perturbation introduced at one grid point to readily travel to the nearest grid points, and thereby eliminate the stationary two-grid-interval waves from the solution. Further justifications for this particular scheme is detailed in Kar (2000) and Kar and Logan (2000).

For implementation of the 2D semi-Lagrangian advection scheme, we need (a) an algorithm to compute the departure points and (b) appropriate horizontal interpolation schemes to interpolate the field variables and other functions from the grid points to the departure point. The departure points are computed following a space and time-centered iterative procedure (Robert 1981). The procedure employs an un-centered linear extrapolation:

$$\Psi^{n-(1-\varepsilon_g)/2} = \tfrac{1}{2}[(3+\varepsilon_g)\Psi^{n-1} - (1+\varepsilon_g)\Psi^{n-2}] \,, \qquad (2.54v)$$

to determine $m[u^{n-(1-\varepsilon_g)/2}, v^{n-(1-\varepsilon_g)/2}]$ at the grid points and a bilinear horizontal interpolation scheme to compute the same at the mid-point of the trajectory. Two to three iterations are generally sufficient for convergence. Aside from this, to interpolate the field variables and other functions from the grid points to the departure points, we have employed a conventional bicubic interpolation scheme.

g. Computational steps for the FISL/SISL schemes

Here we outline the computational steps for time-integration of the hydrostatic model based on the FISL/SISL scheme. Recall that the horizontal and vertical extension of the model domain are shown in Fig. 1 and Fig. 4, respectively. In the following, we use the notations $L_D + 1$, $L_D + 2$, $L_D + 3$, … to denote the rectangular domains $L_D + B_1$, $L_D + B_1 + B_2$, $L_D + B_1 + B_2 + B_3$, …, respectively. Also for convenience, an arbitrary 3D variable or function $\Psi_{i,j,k}$ is simply denoted by Ψ_k. Similarly, at the i-th iteration of the FISL scheme, an arbitrary 3D variable or function $\Psi_{i,j,k}^{n(i)}$ is denoted by Ψ_k^+. The computational steps to be followed for time-integration of the hydrostatic model equations over one time step using the proposed FISL scheme is presented below in the form of a flow chart.

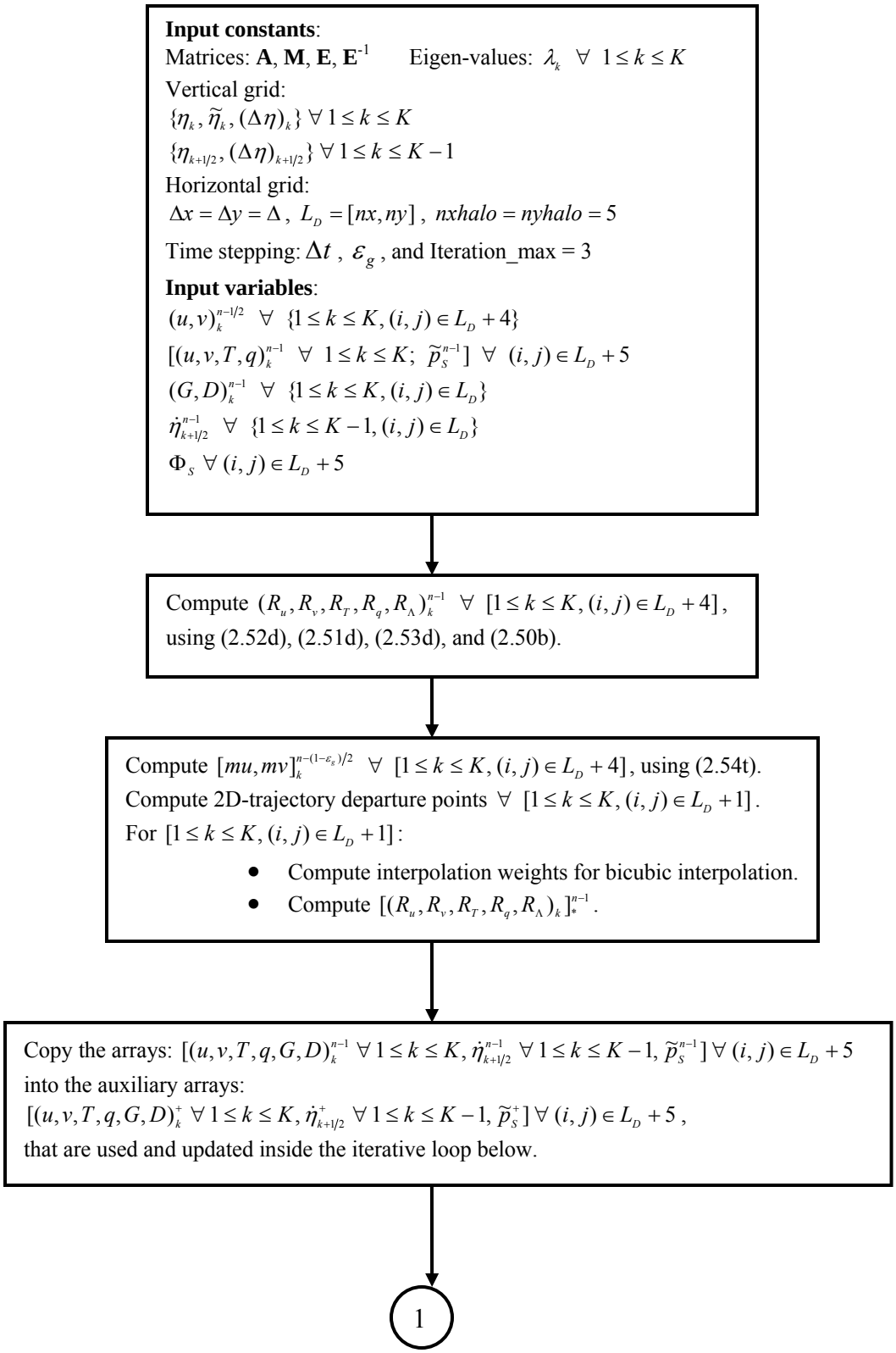
Input constants:
Matrices: **A**, **M**, **E**, **E**$^{-1}$ Eigen-values: $\lambda_k \ \forall \ 1 \le k \le K$
Vertical grid:
$\{\eta_k, \tilde{\eta}_k, (\Delta\eta)_k\} \ \forall \ 1 \le k \le K$
$\{\eta_{k+1/2}, (\Delta\eta)_{k+1/2}\} \ \forall \ 1 \le k \le K-1$
Horizontal grid:
$\Delta x = \Delta y = \Delta$, $L_D = [nx, ny]$, $nxhalo = nyhalo = 5$
Time stepping: Δt, ε_g, and Iteration_max = 3
Input variables:
$(u,v)_k^{n-1/2} \ \forall \ \{1 \le k \le K, (i,j) \in L_D + 4\}$
$[(u,v,T,q)_k^{n-1} \ \forall \ 1 \le k \le K; \ \tilde{p}_S^{n-1}] \ \forall \ (i,j) \in L_D + 5$
$(G,D)_k^{n-1} \ \forall \ \{1 \le k \le K, (i,j) \in L_D\}$
$\dot{\eta}_{k+1/2}^{n-1} \ \forall \ \{1 \le k \le K-1, (i,j) \in L_D\}$
$\Phi_S \ \forall \ (i,j) \in L_D + 5$
Compute $(R_u, R_v, R_T, R_q, R_\Lambda)_k^{n-1} \ \forall \ [1 \le k \le K, (i,j) \in L_D + 4]$, using (2.52d), (2.51d), (2.53d), and (2.50b).
Compute $[mu, mv]_k^{n-(1-\varepsilon_g)/2} \ \forall \ [1 \le k \le K, (i,j) \in L_D + 4]$, using (2.54t).
Compute 2D-trajectory departure points $\forall \ [1 \le k \le K, (i,j) \in L_D + 1]$.
For $[1 \le k \le K, (i,j) \in L_D + 1]$:
• Compute interpolation weights for bicubic interpolation.
• Compute $[(R_u, R_v, R_T, R_q, R_\Lambda)_k]_*^{n-1}$.
Copy the arrays: $[(u,v,T,q,G,D)_k^{n-1} \ \forall \ 1 \le k \le K, \dot{\eta}_{k+1/2}^{n-1} \ \forall \ 1 \le k \le K-1, \tilde{p}_S^{n-1}] \ \forall \ (i,j) \in L_D + 5$
into the auxiliary arrays:
$[(u,v,T,q,G,D)_k^+ \ \forall \ 1 \le k \le K, \dot{\eta}_{k+1/2}^+ \ \forall \ 1 \le k \le K-1, \tilde{p}_S^+] \ \forall \ (i,j) \in L_D + 5$,
that are used and updated inside the iterative loop below.
1

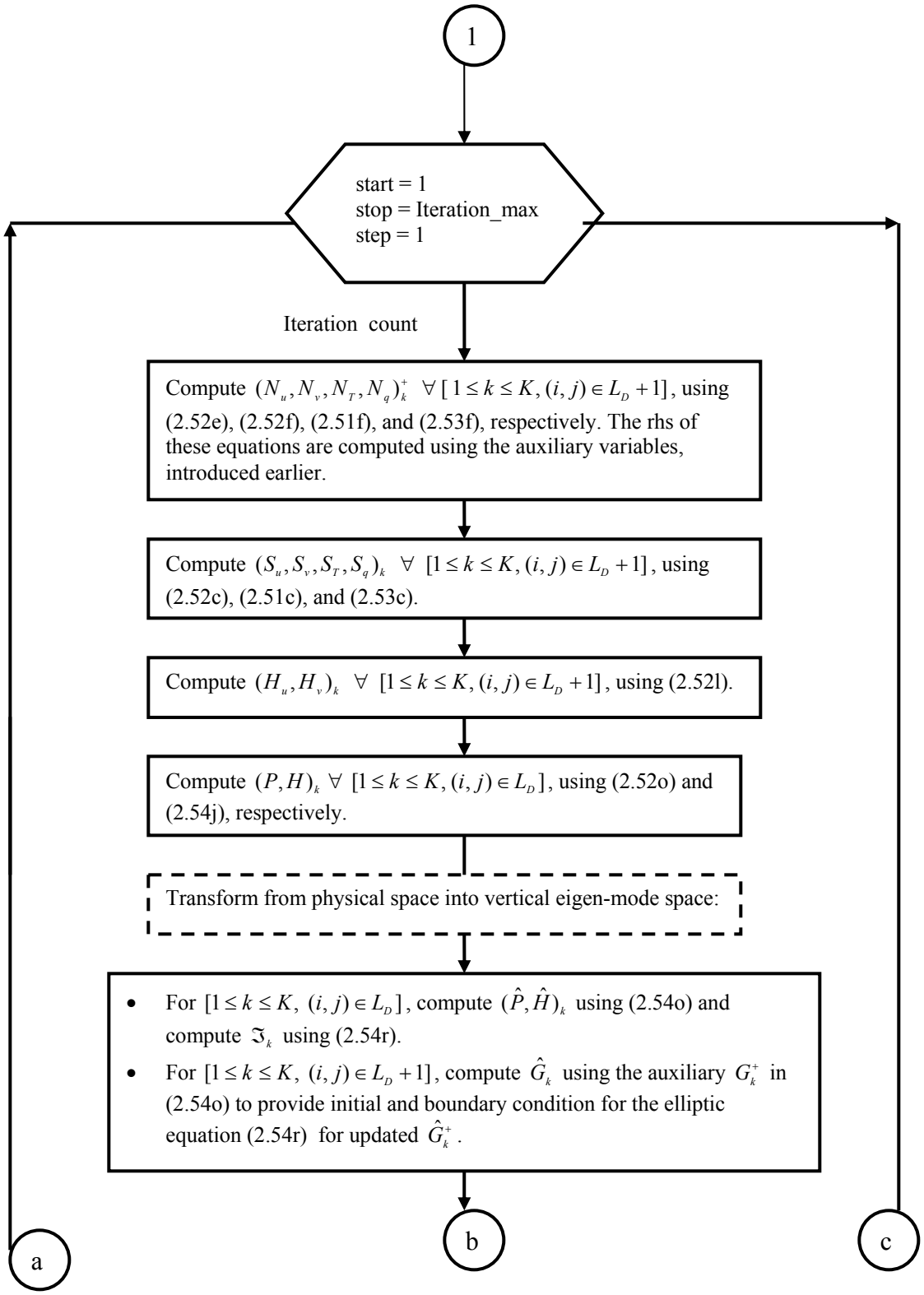
1
start = 1
stop = Iteration_max
step = 1
Iteration count
Compute $(N_u, N_v, N_T, N_q)_k^+ \ \forall\, [1 \le k \le K, (i,j) \in L_D + 1]$, using (2.52e), (2.52f), (2.51f), and (2.53f), respectively. The rhs of these equations are computed using the auxiliary variables, introduced earlier.
Compute $(S_u, S_v, S_T, S_q)_k \ \forall\ [1 \le k \le K, (i,j) \in L_D + 1]$, using (2.52c), (2.51c), and (2.53c).
Compute $(H_u, H_v)_k \ \forall\ [1 \le k \le K, (i,j) \in L_D + 1]$, using (2.52l).
Compute $(P, H)_k \ \forall\ [1 \le k \le K, (i,j) \in L_D]$, using (2.52o) and (2.54j), respectively.
Transform from physical space into vertical eigen-mode space:
For $[1 \le k \le K,\ (i,j) \in L_D]$, compute $(\hat{P}, \hat{H})_k$ using (2.54o) and compute $\Im_k$ using (2.54r).
For $[1 \le k \le K,\ (i,j) \in L_D + 1]$, compute $\hat{G}_k$ using the auxiliary G_k^+ in (2.54o) to provide initial and boundary condition for the elliptic equation (2.54r) for updated $\hat{G}_k^+$.
a
b
c

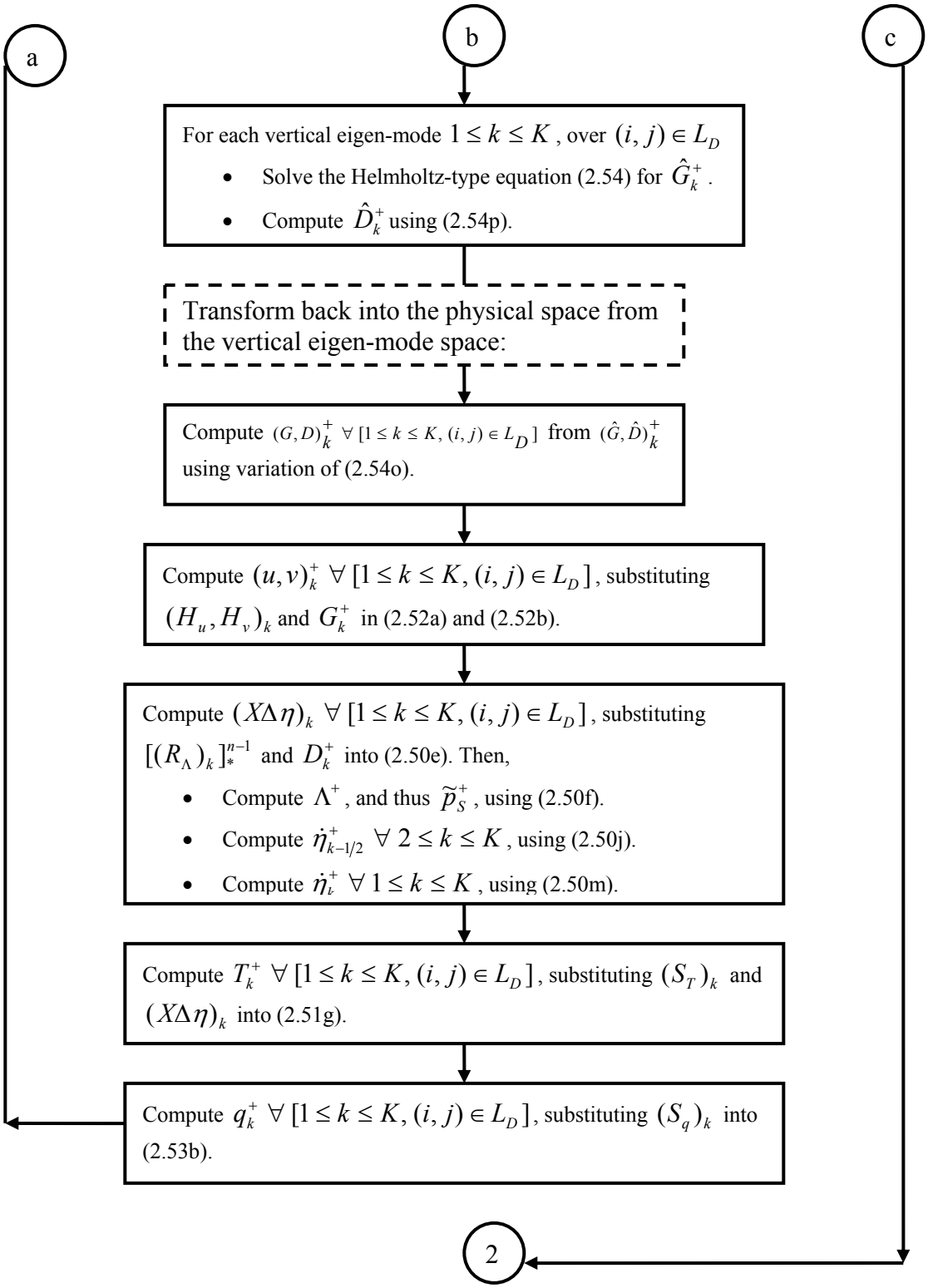
a
b
c
For each vertical eigen-mode $1 \le k \le K$, over $(i, j) \in L_D$
• Solve the Helmholtz-type equation (2.54) for $\hat{G}_k^+$.
• Compute $\hat{D}_k^+$ using (2.54p).
Transform back into the physical space from the vertical eigen-mode space:
Compute $(G, D)_k^+ \ \forall [1 \le k \le K, (i, j) \in L_D]$ from $(\hat{G}, \hat{D})_k^+$ using variation of (2.54o).
Compute $(u, v)_k^+ \ \forall [1 \le k \le K, (i, j) \in L_D]$, substituting $(H_u, H_v)_k$ and G_k^+ in (2.52a) and (2.52b).
Compute $(X\Delta\eta)_k \ \forall [1 \le k \le K, (i, j) \in L_D]$, substituting $[(R_\Lambda)_k]_*^{n-1}$ and D_k^+ into (2.50e). Then,
• Compute Λ^+, and thus $\tilde{p}_S^+$, using (2.50f).
• Compute $\dot{\eta}_{k-1/2}^+ \ \forall \ 2 \le k \le K$, using (2.50j).
• Compute $\dot{\eta}_\iota^+ \ \forall \ 1 \le k \le K$, using (2.50m).
Compute $T_k^+ \ \forall [1 \le k \le K, (i, j) \in L_D]$, substituting $(S_T)_k$ and $(X\Delta\eta)_k$ into (2.51g).
Compute $q_k^+ \ \forall [1 \le k \le K, (i, j) \in L_D]$, substituting $(S_q)_k$ into (2.53b).
2

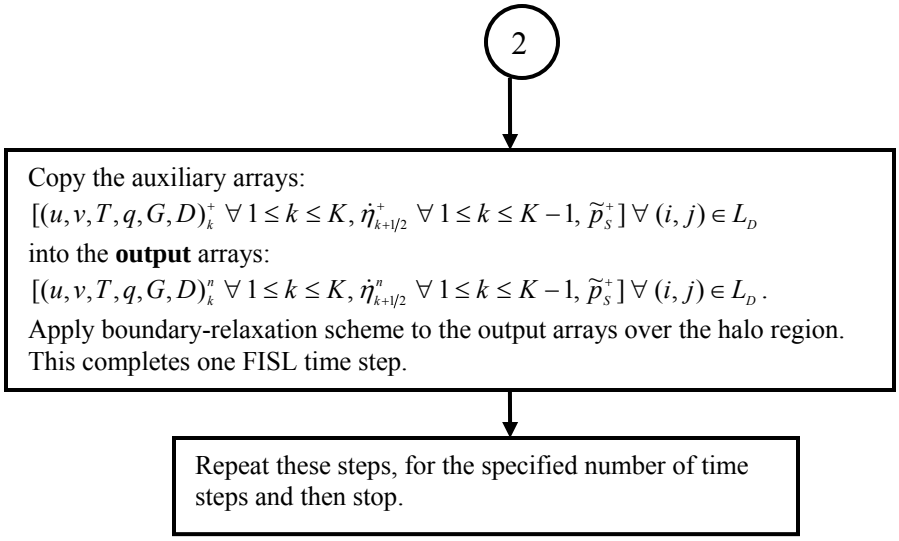

3. NUMERICAL SIMULATION

The FISL model is at its early stage of development and various tests are being performed to debug the model code and check the effectiveness of the model formulation. Thus, the results presented here are only preliminary. Recently, we employed the model to simulate the nonlinear evolution of mid-latitude disturbances. To this end, the model domain is horizontally reduced to a cyclic-in-*x*, mid-latitude β-plane channel. The pressure at the model top is set to 1 hPa, with 41 uniformly spaced layers in the vertical. The length and width of the β-channel are 4000 km and 10000 km, respectively. The horizontal grid size, uniform in *x* and *y*, is 100 km. There are five grid points in the *x* and *y* halo regions. The reference isothermal atmosphere is set to 330 K. The initial condition consists of a zonally uniform geostrophically balanced basic state and small-amplitude random perturbations in the temperature and surface pressure fields superimposed on the basic state.

For this simulation, we have included a Newtonian heating term in the thermodynamic energy equation that relaxes the temperature to an equilibrium state. Thus, the heating term is given by

$$Q_k / c_{pd} = \gamma_k (T^* - T)_k , \qquad (3.1)$$

where γ_k assumes constant specified values and $T^*{}_k(y)$ is the zonally uniform equilibrium temperature.

We have also included Rayleigh-damping type friction terms in the (u, v) momentum equations, given by

$$(F_x)_k = -(C_x)_k |u_k| u_k ,$$
$$(F_y)_k = -(C_y)_k |v_k| v_k , \qquad (3.2)$$

with $(C_x, C_y)_k$ defined by

$$(C_x)_k = (C_y)_k = (10\tau_k)^{-1} , \qquad (3.3)$$

where τ_k assumes constant specified values. We have included such simple thermal forcing and friction terms, because the model does not include comprehensive physical processes at this stage. However, a dry convective adjustment is included in the model to restore a neutral stratification between adjacent unstable layers when necessary. The heating parameters are set at $\gamma_k = 10$ days for $2 \le k \le K$ and $\gamma_1 = 1$ day. The friction is applied only at the lowest four levels with $\tau_1 = 0.5$ day. Note that the lowest four layers add up to an approximate thickness of 100 hPa.

The FISL scheme employs a time step of 20 min, with 3 outer iterations and $\varepsilon_g = 0$. To remove some residual grid-scale noise from the solutions, a horizontal 2D filter is used at each time step. There is no other explicit damping or diffusion used in the present simulation.

The model is integrated for 20 days. The model predicted surface pressure together with the potential temperature at level 1 for days 6 to 20 is presented in Fig. 5. The geopotential height and the potential temperature at level 21 for the same time period are shown in Fig. 6. Note that initially, the levels 1 and 21 are located at 988 hPa and 500 hPa, respectively. Early stages of development (days 6 and 8) shows two unstable waves with wavelengths of approximately 1000 km and 4000 km. However, starting at day 12, a single domain-size long wave dominates. Frontal zones develop at the surface and the upper troposphere. Well-defined fronts develop at the surface and upper troposphere; the disturbance continues to grow and the low pressure center deepens until day 16. Both low and high pressure maxima begin to weaken after day 16.

Clearly, the model is able to simulate the nonlinear evolution of a mid-latitude disturbance on the β-plane. We have found that such simulations are indeed sensitive towards the prescription of initial condition and the parameters related to heating and friction. We are currently addressing such issues.

4. CONCLUSIONS

A fully-implicit, semi-Lagrangian, 3D hydrostatic, limited-area, grid-point model has been developed at NCEP/EMC. We are currently testing the model to simulate the nonlinear evolution of a mid-latitude disturbance on the b-plane. We are also applying the model in a vertical (x, η) slice version to simulate linear and nonlinear hydrostatic mountain waves over idealized mountain shapes. Preliminary results will be presented at the conference.

ACKNOWLEDGMENTS

The author would like to thank Dr. Celal Konor for his continued assistance in the simulation and understanding of frontogenesis using the FISL/SISL model.

REFERENCES

Kar, S. K., 2000: Stable centred-difference schemes, based on an unstaggered A grid, that eliminate two-grid interval noise. *Mon. Wea. Rev.*, **128**, 3643-3653.

Kar, S. K., and L. W. Logan, 2000: A semi-Lagrangian and semi-implicit scheme on an unstaggered horizontal grid. *Aust. Met. Mag.*, **49**, 293-317.

Lin, C.A., Laprise, R. and Ritchie, H. 1997: *Numerical methods in Atmospheric and Oceanic Modelling: The Andre J. Robert Memorial Volume*. NRC Research Press, 581 pp.

Phillips, N. A., 1957: A coordinate system having some special advantages for numerical forecasting. *J. Meteor.*, **14**, 184-185.

Robert, A. J., 1981: A stable numerical integration scheme for the primitive meteorological equations. *Atmos. Ocean.*, 19, 35-46.

Saad, Y., 2003: *Iterative Methods for Sparse Linear Systems*. 2d ed. SIAM, 528 pp.

Yeh, K.-S., J. Cote, S. Gravel, A. Methot, A. Patoine, M. Roch, and A. Staniforth, 2002: The CMC-MRB Global Environmental Multiscale (GEM) Model. Part III: Nonhydrostatic formulation. *Mon. Wea. Rev.*, 130, 339-356.

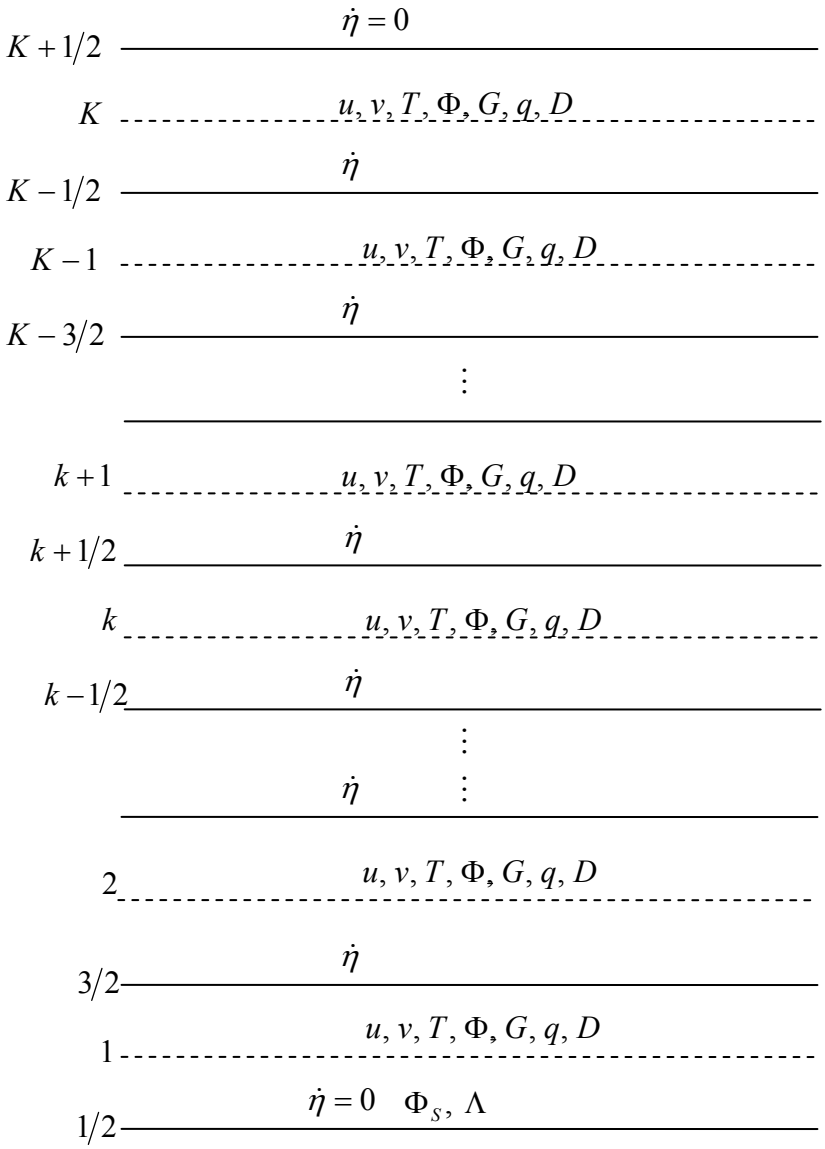

Figure 1. Vertical grid and distribution of variables.

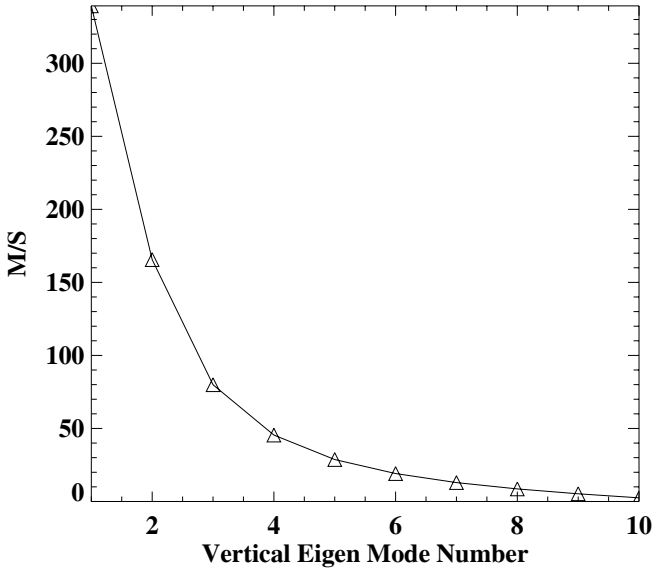

Figure 2. The pure gravity wave speed (m s^{-1}) of the vertical eigen-modes of a 10 layer version of the FISL/SISL 3D hydrostatic model. The reference atmosphere is isothermal (300 K), and the vertical layers are of uniform thickness.

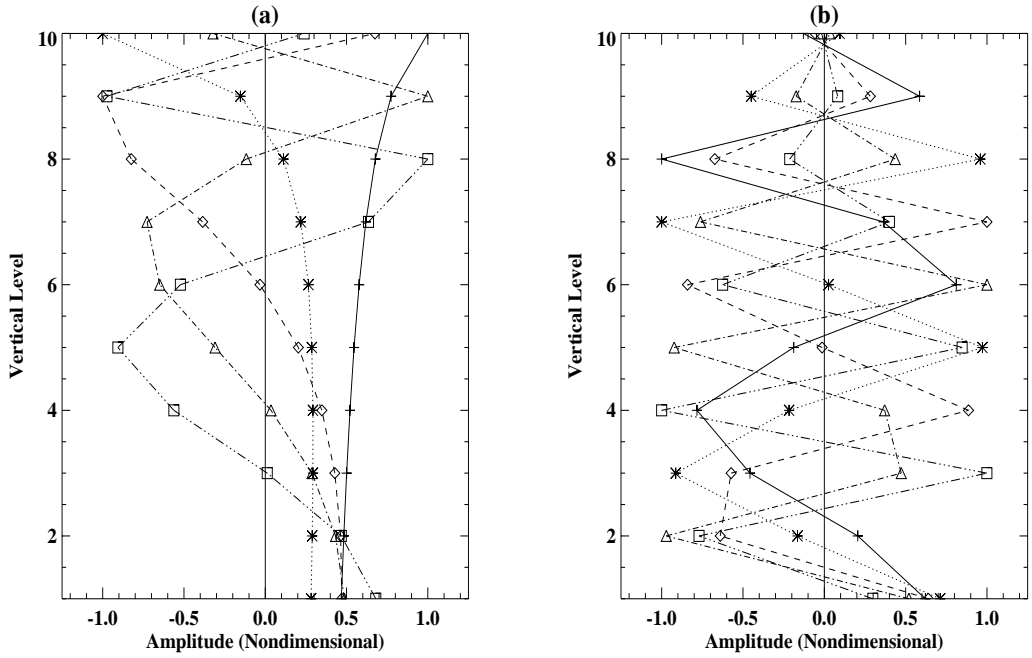

Figure 3. Non-dimensional amplitudes of the vertical eigen-vectors of the FISL/SISL 3D hydrostatic model are plotted as a function of the vertical levels. The curves with the embedded symbols (+, *, ◊, Δ, and □) correspond respectively to the eigen-modes 1-5 in (a) and 6-10 in (b).

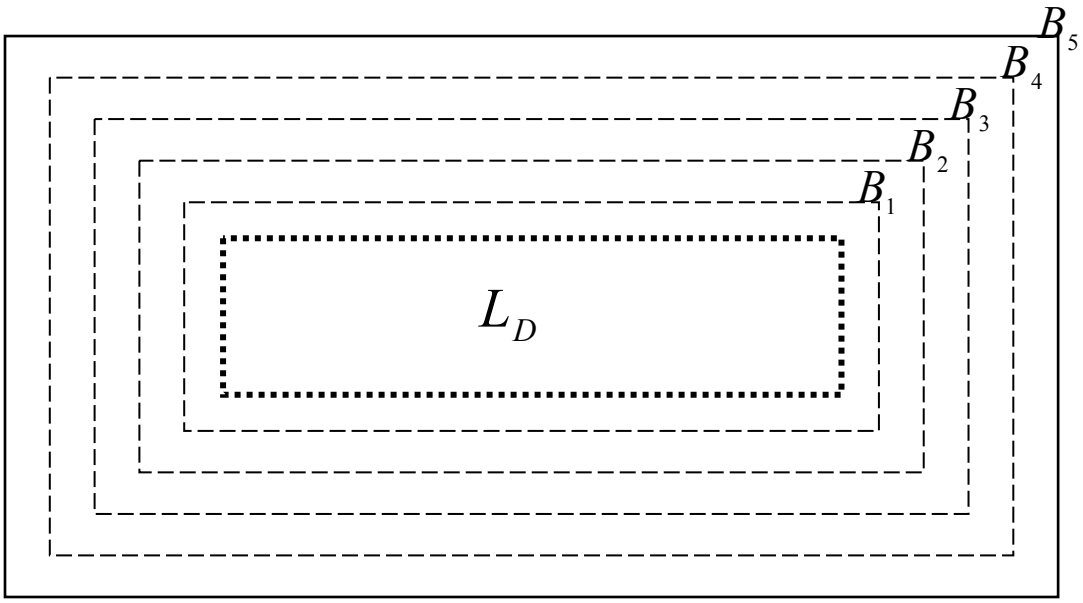

Figure 4. A schematic of the horizontal limited-area computational domain. The innermost subdomain is denoted by L_D. The dashed-line rectangles B_1, B_2, B_3, and B_4 represent the first four lines of grid points surrounding L_D. The solid-lined rectangle B_5 represents the lateral boundary of the limited area.

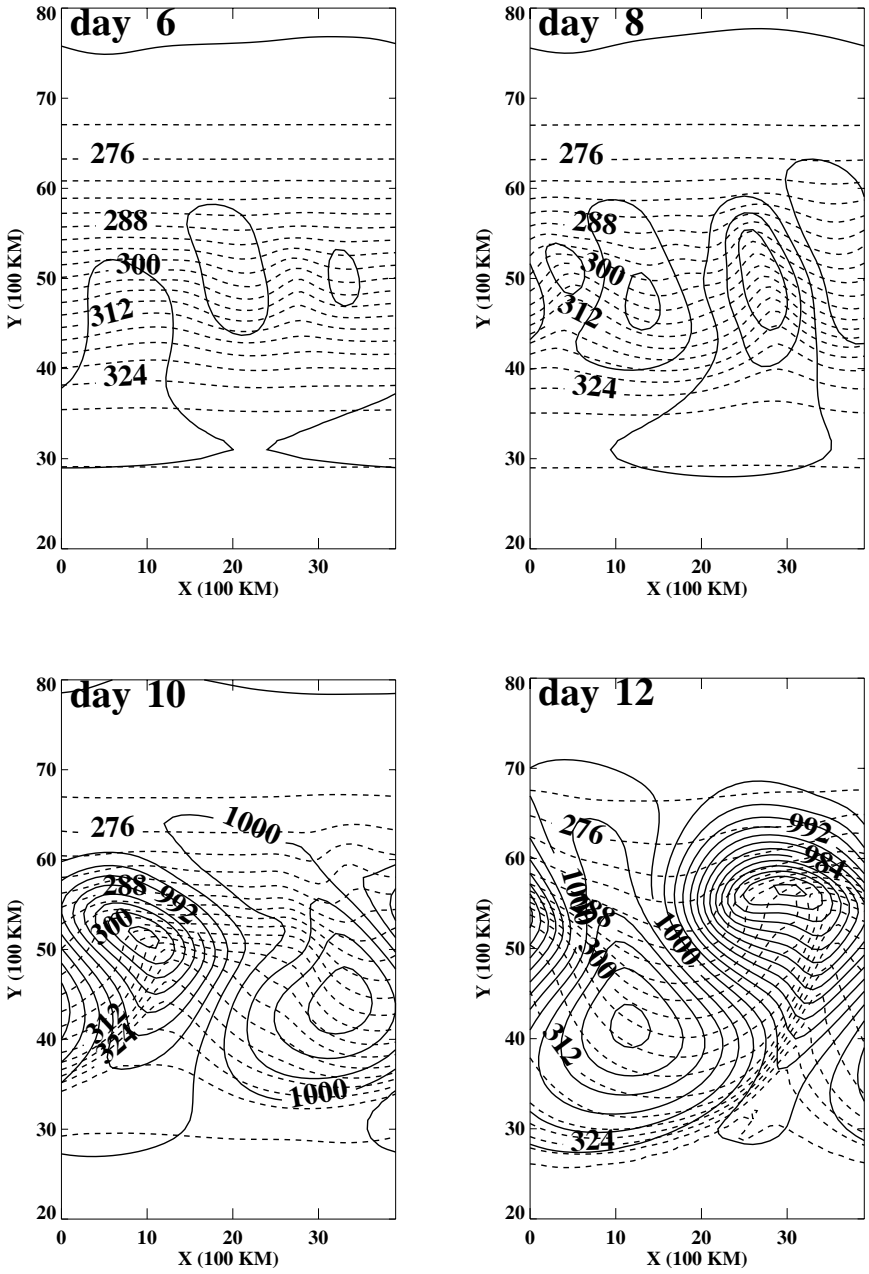

Figure 5. Surface pressure (solid lines) and the potential temperature (dashed lines) at the lowest model level for day 6 to day 12. Contour intervals are 2 hPa for surface pressure and 3 K for potential temperature.

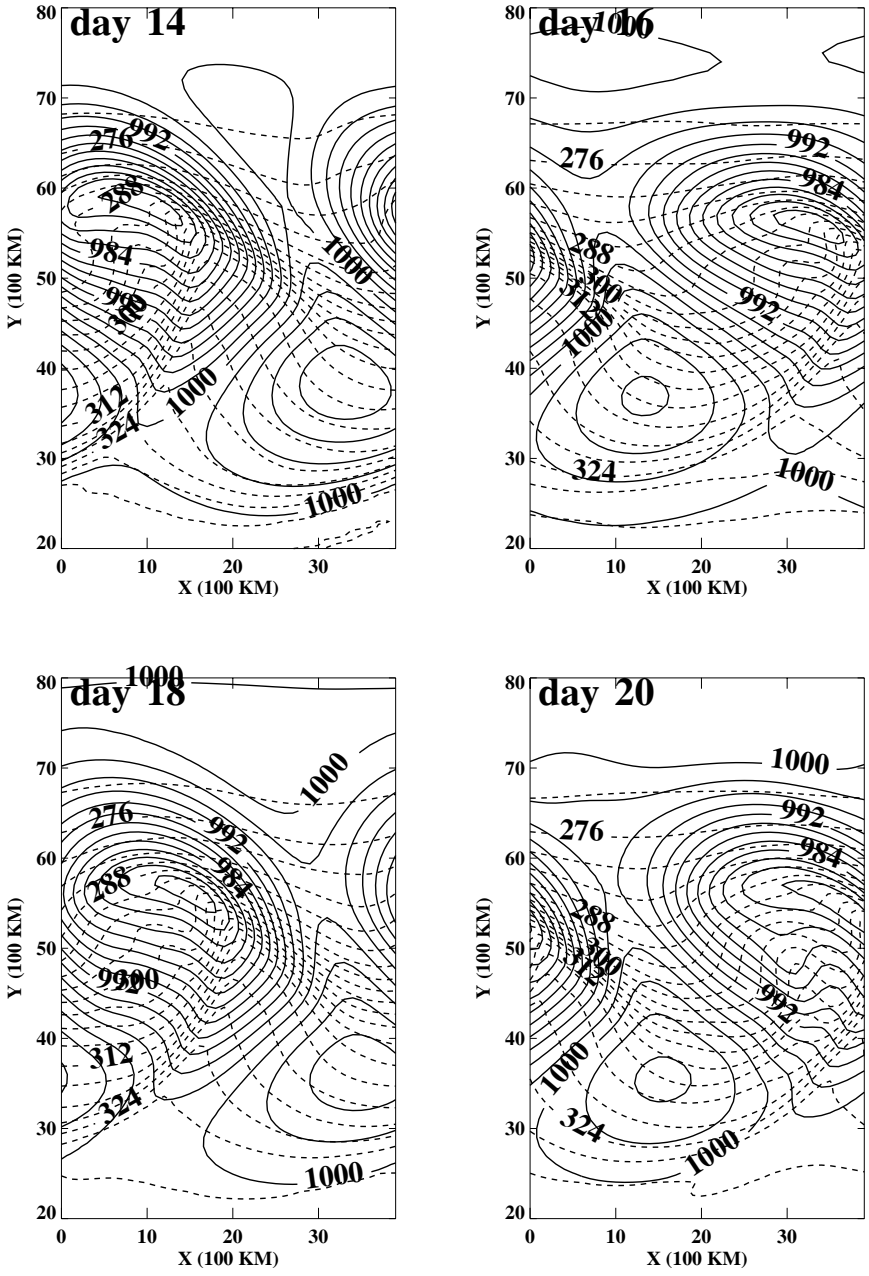

Figure 5. (*Continued*)

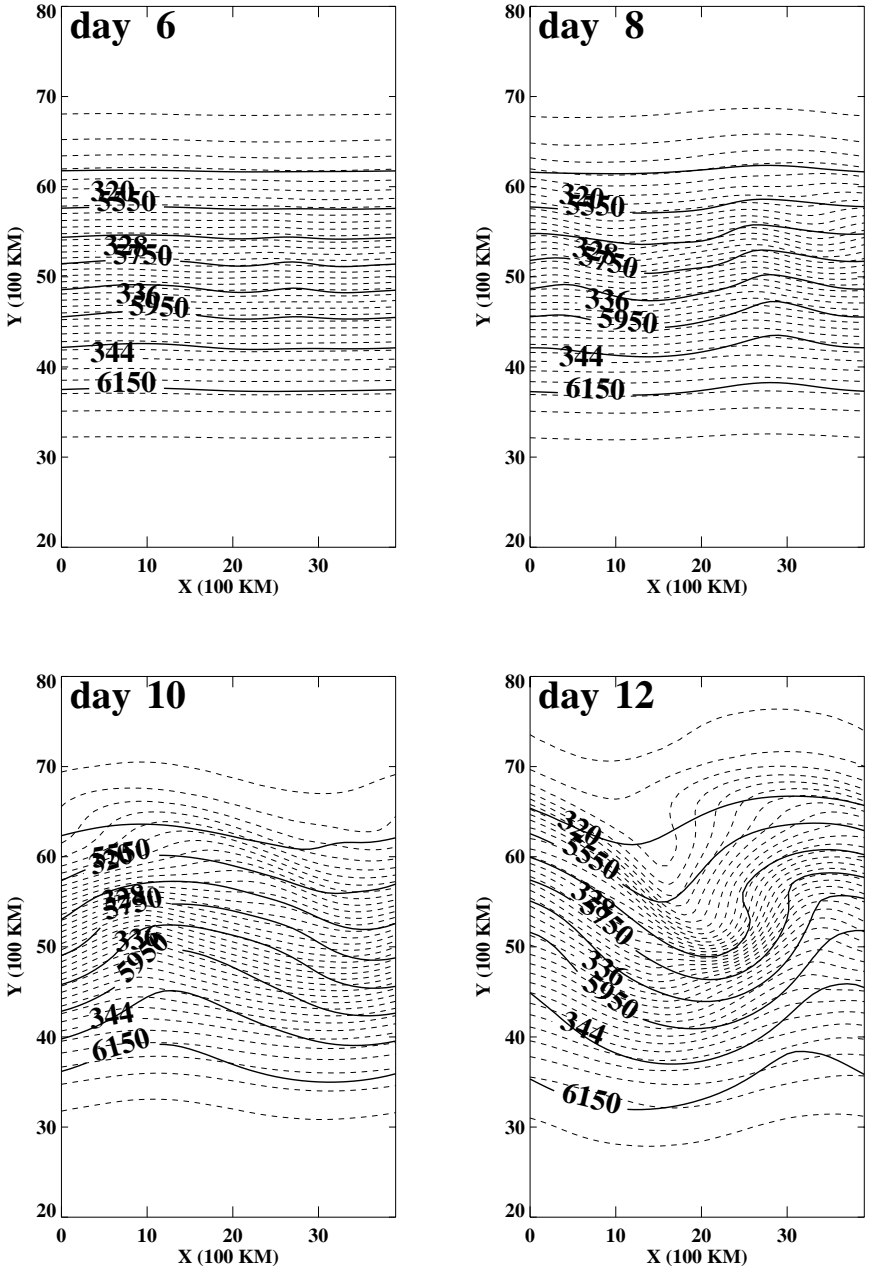

Figure 6. Geopotential height (solid lines) and the potential temperature (dashed lines) at the model level 21 for day 6 to day 12. Contour intervals are 100 gpm for geopotential and 1 K for potential temperature.

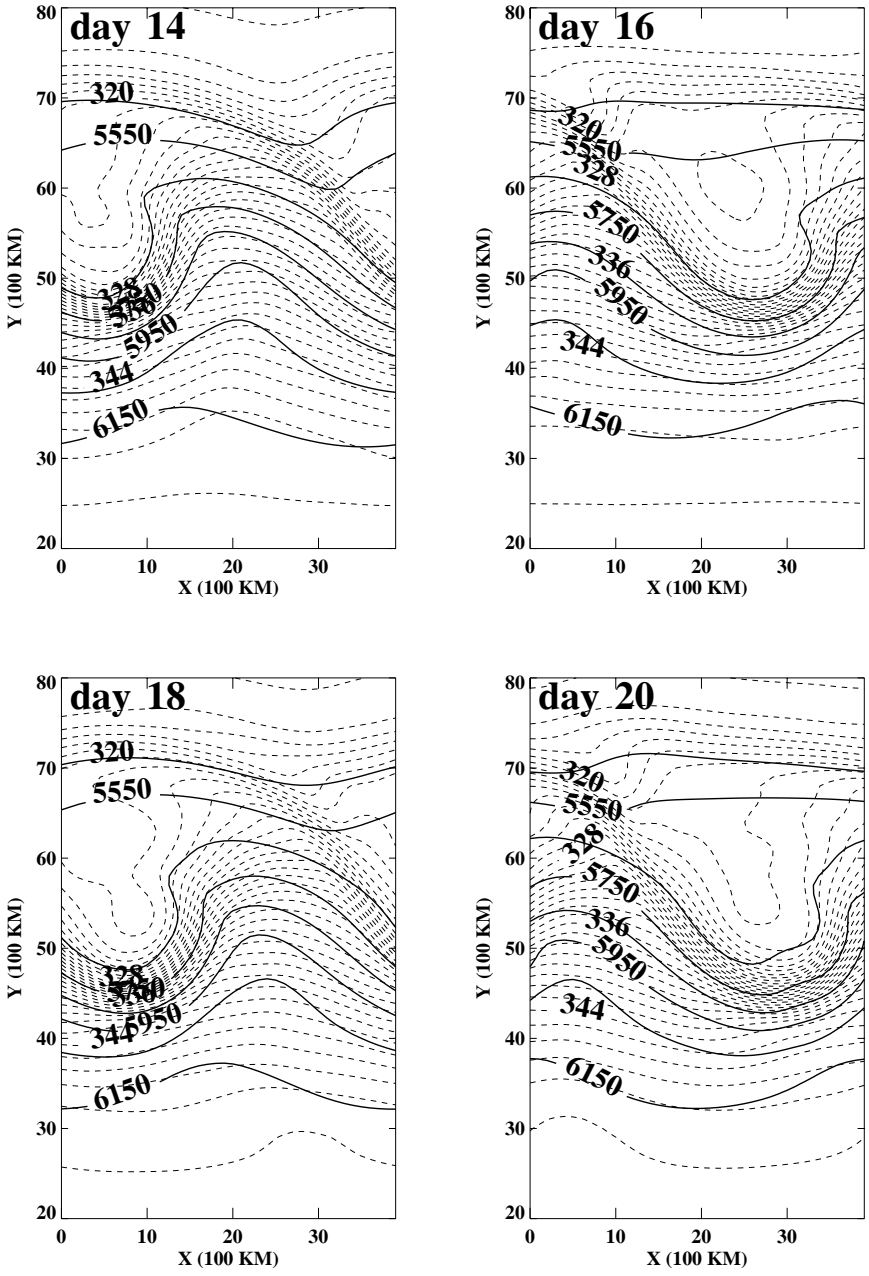

Figure 6. (*Continued*)

[i] Corresponding author address: Sajal K. Kar, W/NP2 RM 207, WWBG, 5200 Auth Road., Camp Springs, MD 20746-4304
Email: Sajal.Kar@noaa.gov